Energy & Buildings 324 (2024) 114874

Contents lists available at ScienceDirect

Energy & Buildings

journal homepage: www.elsevier.com/locate/enb

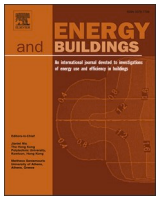

Evaluation of aerial thermography for measuring the thermal transmittance (U-value) of a building façade

Marta Videras Rodríguez [a], Sergio Gómez Melgar [b,*], José Manuel Andújar Márquez [b]

[a] Programa de Doctorado de Ciencia y Tecnología Industrial y Ambiental, Centro de Investigación en Tecnología, Energía y Sostenibilidad – CITES (Research Centre for Technology, Energy and Sustainability), Universidad de Huelva, Campus El Carmen, 21071, Huelva, Spain
[b] TEP192 Control y Robótica, Centro de Investigación en Tecnología, Energía y Sostenibilidad – CITES (Research Centre for Technology, Energy and Sustainability), Universidad de Huelva, Campus La Rábida, Palos de la Frontera, 21071, Huelva, Spain

ARTICLE INFO

Keywords:
U-value
Aerial thermography
Thermometric method
Building envelope
Unmanned aerial vehicle
Energy efficiency

ABSTRACT

In efforts to mitigate greenhouse gas emissions in the construction sector, policies promoting energy efficiency improvements in existing buildings are being implemented. Accurately assessing the impact of energy retrofit strategies requires precise determination of thermal envelope performance through energy audits. Aerial thermography, employing unmanned aerial vehicles (UAVs) equipped with infrared thermal cameras (IRT), is an underused method overcoming limitations in energy audits of large buildings or complexes. This approach offers an elevated perspective, providing an overview of the building's thermal patterns, aiding in the identification of thermal envelope defects. By measuring temperature distribution, even in inaccessible envelope areas, the severity of identified defects can be estimated. Beyond detecting thermal bridges, air leaks, and moisture, aerial thermography is valid for estimating thermal transmittance (U-value) of enclosures. The aim of this research is to evaluate this method to calculate the U-value of the façade of an university building located in a Subtropical Mediterranean climate, during a typical full day in different seasons of the year. Concurrently with aerial thermography, the thermometric method (THM) was applied to compare results and refine the operational conditions during U-value measurement using different statistical indices and uncertainty analysis. The results demonstrated the validation of airborne thermography as a method for U-value calculation under specific meteorological and operational conditions, overcoming the common physical limitations of traditional building audit methods.

1. Introduction

Currently, since buildings account for 40 % of the European Union's final energy consumption, it is essential to reduce the use of non-renewable energy in the construction sector to mitigate greenhouse gas emissions (GHG) [1]. The main actions to reduce GHG in the construction sector are structured around two basic guidelines: regulatory development aimed at greater efficiency and energy savings in buildings, and the implementation of active policies to promote energy improvement in existing buildings and high-energy efficiency in newly constructed buildings [2]. Although building regulations are becoming more demanding in terms of sustainability for new buildings, there is a large stock of buildings that were constructed under less stringent sustainability regulations. Approximately 55 % of the building stock in Spain predates the year 1980, and 21 % of it is over 50 years old [3].

For this reason, energy retrofitting of existing buildings is key to reducing pollution levels in the building sector, as it adapts the energy efficiency level of these buildings to current requirements. Successful energy retrofitting requires ensuring that the level of efficiency is maintained throughout the life cycle of the building [4]. The energy consumption of the existing building stock depends mainly on the characteristics of the construction and the use of building installations. Building retrofit strategies focus on these two areas: passive actions, intervening on the building envelope to improve its thermal insulation and air tightness, and active actions, replacing ventilation, heating, and cooling (HVAC) and lighting systems with high-efficiency equipment, combined with the investment of renewable energy technologies [5]. The most important factors for increasing the energy efficiency of a building can be summarised as improving the thermal insulation performance of the building envelope and building equipment in

* Corresponding author.
E-mail addresses: marta.videras245@alu.uhu.es (M. Videras Rodríguez), sergomel@uhu.es (S. Gómez Melgar), andujar@uhu.es (J.M. Andújar Márquez).

https://doi.org/10.1016/j.enbuild.2024.114874
Received 28 May 2024; Received in revised form 20 September 2024; Accepted 3 October 2024
Available online 5 October 2024

combination with changing the user's consumption habits [6].

The strategies aimed at improving the building envelope are approached from the perspective of heat transfer through the building envelope. The building envelope, consisting of facade walls, windows, and roof, separates the interior of the building from the exterior, protecting the habitable space from external weather conditions such as wind, rain, or solar radiation. The heat transfer rate of the envelope depends mainly on the thermal conductivity of its component materials [7]. Thermal conductivity measures the ability to transfer heat through a material when there is a temperature difference between two points (indoor and outdoor). The type of materials used, the construction process of the envelope and the deterioration it undergoes when exposed to climatic conditions lead to the presence of thermal defects such as thermal bridges, air leakage and dampness. The presence of thermal bridges may contribute 23 % to the total heat loss through envelope transmission [8]. These thermal defects play a crucial role in the energy consumption of buildings contributing to 30 % of the energy efficiency loss of residential buildings in Europe [9,10].

Through the building envelope, heat losses occur in winter and undesired heat gains happen in summer, negatively impacting the building's energy consumption [11]. In cold climate zones, heat transfer from the building envelope may account for 50 % of the annual energy consumption for heating public buildings [12]. A survey of 135 dwellings in Boston revealed that air leakage in the envelope accounts for almost 40 % of the energy lost in heating a residential building [13]. In warm climate zones, the addition of 50 mm of thermal insulation in the vertical envelope to reduce heat gains from the outside through the envelope could reduce cooling consumption by 25 % [14]. Increasing thermal insulation is an effective method of improving the thermal performance of opaque building envelopes [15]. Thermal insulation stands out as one of the most effective methods for decreasing energy usage, whether it be for winter heating or summer cooling [16,17]. However, improper design of the thermal insulation can lead to reduced heat losses during the heating season and incorrect overheating during the cooling season [18].

To assess the impact of potential energy retrofit strategies for existing building envelopes is essential to accurately determine the current state of thermal envelope performance. Energy auditing serves as a fundamental tool with the primary objective of analyzing and diagnosing a building's energy flow to determine its consumption and propose options for reduction, leading to consequent economic and energy savings. As part of the energy audit of a building, the assessment of envelope performance is conducted on-site by analyzing its characteristics, calculating the thermal transmittance (also called U-value) of the building's enclosures and detecting thermal bridges, air leaks, and dampness through the blower door test [19]. On-site measured information gathered during an energy audit can prove highly beneficial for calibrating building energy models (BEM) using simulation software, aiming to reasonably estimate energy savings following envelope retrofitting [20].

Infrared thermography (IRT) is a widely employed tool in the construction sector for assessing the thermal performance of the building envelope, as it is useful for the visualization of thermal defects and the estimation of the U-value of the envelope [21,22,23]. Qualitative infrared thermography is a practical diagnostic tool used to detect defects in the building envelope such as heat loss, missing or damaged thermal insulation of walls and roofs, thermal bridges, air leakage and sources of dampness [9]. Quantitative infrared thermography is used in building energy audits to measure the U-value of the façade, the U-value of the roof, the U-value of windows and glazing systems and the assessment of the emissivity of building materials [24]. Generally, this methodology is applied using infrared thermal cameras at ground level from inside or outside the envelope. In outdoor inspections, the main limitations of ground-based thermography are due to the inaccessibility of capturing images of the façade of tall buildings and the expense of operator time in capturing images of large sets of buildings. For this reason, aerial thermography, performed with infrared thermal cameras mounted on UAVs (unmanned aerial vehicles), is proposed as a methodology with significant advantages over ground-based thermography, although its use is currently infrequent [25].

Recent research has assessed the thermal performance of building envelopes calculating the U-value of the building's envelopes through aerial thermography. Aerial thermography carried out with infrared thermal (IRT) cameras equipped on UAVs (unmanned aerial vehicles) allows the collection of IRT images accurately, quickly and with minimal security risks for building energy efficiency and urban sustainability tasks [26,27,28]. In the field of quantitative aerial thermography, the scientific community has proposed methodological frameworks for calibrating building energy models. Bayomi et al. performed an on-site measurement (in spring, early in the morning) with an infrared camera equipped on a UAV to quantify the percentage of thermal bridges and the U-value of the envelope of a whole building undergoing energy retrofitting. The results were used to calibrate a building energy model and the proposed method was validated by comparing the real energy consumption of the building with the simulated energy consumption based on the calculated U-value and the design U-value [29]. Recently, Benz et al. proposed a methodological framework for estimating the U-value of thermograms obtained using UAVs for the subsequent simulation of the thermal energy of a building. In this research, a single predawn measurement was also performed although the time frame for the flight was previously determined using surface temperature sensors installed in the envelope. The time of highest thermal gradient between indoors and outdoors was chosen [30]. Rakha et al. applied aerial thermography to survey the thermal envelope of different buildings during a winter day in two consecutive flight missions to perfect the procedure [31].

Based on the literature review, aerial thermography is presented as a method that overcomes limitations present in energy audits of large buildings or clusters of buildings. Applied qualitatively, aerial thermography allows the visualization of thermal patterns to identify areas with defects more efficiently than conventional methods by providing an overview of the whole building from a high perspective. When applied quantitatively, it allows estimating the severity of identified defects by measuring the temperature distribution even in areas of the envelope inaccessible from the ground (such as facades of high-rise buildings or roofs). However, gaps have been identified in the literature on the application of this methodology in a long-term test, at different times of the day and in various seasons of the year for the quantification of the U-value. The results obtained from a single measurement may not be representative taking into account possible errors derived from the measurement process (such as the acquisition of out-of-focus images) and weather conditions during operation.

To validate this methodology, it is necessary to deepen the test duration by performing longer experiments with a higher frequency of data collection. This research applied aerial thermography continuously during all hours of a full day in different seasons of the year to validate this U-value calculation methodology and provide a baseline to facilitate its applicability to other buildings. This research aims to overcome the physical limitations of traditional building audit methods, such as the inspection of tall building facades and access to inaccessible areas on foot, as well as the review of large groups of buildings. By ensuring operator safety and reducing inspection time between different areas or buildings, the frequency of measurements in different areas or buildings may be increased.

The experiment was conducted using a UAV equipped with an IRT camera that acquired thermal images of a building envelope for calculating its U-value during a typical winter day and a typical summer day. To validate the method, the thermometric method (THM) was simultaneously applied to compare the results and to limit the test duration by evaluating the operating conditions during the U-value measurement. While the thermometric method lasted 60 h (three nights and two days) taking measurements every ten minutes, the aerial thermography was

performed during a diurnal cycle (24 h) recording measurements every ten minutes. The building envelope of the analyzed building corresponds to the typical constructive characteristics of existing buildings in Southern Europe composed of brick walls without thermal insulation. The data presented in this document are derived from the analysis of a single wall that has the same characteristics in terms of thickness and material composition as the rest of the building's façades.

The article is structured as follows: the study site, the data acquisition and post-processing method and the thermometric and thermographic methodologies used are presented in detail in section 2; the results obtained in the experimentation using both methods in winter and summer are shown in section 3; these results are analyzed, compared and discussed in section 4; ending the research with the conclusions obtained during the experimentation which are presented in section 5.

2. Materials and methods

2.1. Available methodologies for thermal transmittance measurement (U-value)

The thermal transmittance or U-value (W/m^2K) defines the amount of heat that flows through the envelope due to the temperature difference between the two spaces it separates [32]. The scientific community has analyzed the different existing methodologies to calculate the U-value [33,34]: the theoretical method, the heat flow meter method (HFM), the simple hot box-heat flow meter (SHB-HFM), the temperature based or thermometric method (TBM or THM) and the quantitative infrared thermography (IRT).

The theoretical calculation defined in ISO 6946 [32] is a fast and cost-effective approach that requires accurate information on the envelope typology and the thickness and thermal conductivity of each envelope material to obtain reliable results [35]. It is a calculation method that does not require a measurement campaign and is usually calculated during the development of the construction project. Some investigations compared this approach with other conventional in-situ measurement methods such as the HFM. In historic brick masonry buildings, the theoretically calculated values overestimated the in situ measured values; while in contemporary and sustainable buildings, the theoretical method calculated lower U-values than the measured values [36,37]. The discrepancies between the theoretically calculated values and the measured in situ values indicated that continuous in situ measurements are necessary to assess the U-value in order to obtain accurate information on the degradation of envelope thermal performance [38].

The heat flow meter (HFM) is a non-destructive method (NDT) and standardized according to ISO 9869–1 [39], whose U-value quantification procedure is based on the direct measurement of the heat flow rate and temperatures on both sides of the enclosure under stationary conditions. It requires a heat flow meter which is placed on the surface of the element with the most stable temperature (indoor) and two indoor and outdoor ambient temperature sensors. According to the standard, the temperature difference must be greater than 10 °C and remain constant for as long as possible [39]. Generally, a weather station is also used to monitor environmental conditions and an infrared camera is used to ensure that the heat flow meter is installed on a surface without thermal defects [33]. This method is often applied in conjunction with qualitative thermography to support the measurements [40,41].

Since stationary conditions do not occur in practice, the standard suggests three methods: the average statistical method which uses the average of the observed U-values over a sufficiently long time (days or weeks), the dynamic statistical method which requires less analysis time but more complex calculations, and the hot-box and cold-box method which is performed under laboratory conditions and allows controlling temperatures during experimentation [34]. Research comparing the average statistical method with the dynamic method has shown variations of less than 10 % between the two methods considering the possibility of reducing the in situ measurement period [38]. Compared to the theoretical method, the differences in the U-values calculated with the dynamic method were lower than the values obtained with the average statistical method [42]. The regulation suggests that measurements should be carried out for at least three days as long as the temperature around the HFM is stable and the consecutive measurements do not differ more than 5 %. Otherwise, the experimentation should be extended for more than seven days [39].

Despite the widespread use of the HFM method, the literature has shown that this method is sensitive to the operating conditions under which the measurement is performed such as the correct installation of the heat flux meter and the climatic conditions during the experimentation. Authors have shown uncertainties related to the estimation of the U-value associated with climatic conditions: 8 % under optimal operating conditions and 50 % under non-optimal conditions (performed in the summer season) [43]. The season of the year and the orientation of the enclosure is crucial in the estimation of the U-value, showing a variation with respect to the theoretical U-value of 20 % for a north-facing wall in summer and a variation of 60 % for a south-facing wall in winter applying the HFM method, concluding the unfeasibility of carrying out this experiment on enclosures exposed to direct solar radiation [44]. It is recommended to place the sensors on north-facing facades to exclude the impact of solar radiation on the external surface and away from internal heat sources [45].

The simple hot box-heat flow meter method (SHB-HFM) is a method based on ISO 8990 [46], which estimates the U-value using the HFM method and provides a stable thermal environment by maintaining a constant temperature difference over time between indoors and outdoors. It consists of a temperature control box that is installed on the surface with the highest temperature (inside in winter and outside in summer) to establish and maintain the temperature difference between the two environments separating the enclosure [47].

The thermometric method (THM) also called temperature-based method (TBM) or air-surface temperature ratio (ASTR), is a non-standardized method widely used by the scientific community for in situ U-value measurements. It is a method that requires minimal instrumentation: two sensors to measure the indoor and outdoor air temperature, three probes to measure the surface temperature of the interior wall and a data logger [48]. Like other non-destructive methods, it requires temperatures to remain constant over time, avoiding fluctuations and ensuring a thermal difference between the interior and exterior of 15 °C. The same conditions as with the HFM method must be considered: avoiding direct solar radiation on the envelope and conducting the experimentation in a section in good conservation conditions without thermal bridges. The measurement should last for a minimum of three days of experimentation, which can be extended if it is a heavy wall or reduced if it is a light wall [39]. This method is a promising technique with advantages in terms of speed, simplicity and price compared to the HFM method. The validity of the results of this method is not affected when there is a large temperature difference between indoors and outdoors and the thermal conditions remain stable [49].

This methodology is included in commercial equipment sold for the purpose of calculating U-value and in low-cost equipment developed by the scientific community [50,51]. This research team developed a THM-based meter that demonstrated differences of less than 2 % in the measurement of U-value using simultaneously the HFM method [52]. Both methods were evaluated over long periods of time (seven days) and short periods of time (four hours, between 02:00 am and 06:00 am) demonstrating an error rate of 2.6 % concluding the feasibility of applying the THM method in short periods of time [53]. Other experiments carried out in a Mediterranean climate demonstrated the validity of the THM method in winter, with associated uncertainties between 6–13 % with respect to theoretically calculated values, while in summer the results were not valid due to the uncertainty associated with the test [48].

The quantitative infrared thermography (IRT) is a non-destructive method standardized according to ISO 9869–2 [54], used for the calculation of the U-value. The basic principle of this methodology consists of measuring the amount of irradiance of an envelope that is in contact with the outside air by using an IR camera to measure the indoor surface temperature of the wall, the emissivity of the material and the reflected temperature of the surroundings. The methodology requires very specific environmental conditions to achieve close-to-steady-state conditions. It is necessary to avoid the direct influence of fans and heating or cooling devices on the surface to be measured, to free up the measurement area to avoid visual interference that would obstruct the field of view of the infrared camera. It is also necessary to ensure that the difference between indoor and outdoor temperature is greater than 10 °C [54]. The standard specifies that the timing of the experimentation depends on factors such as climatic conditions or type of construction. In general, it is recommended that the measurement should be carried out at night and should last long enough to capture significant variations in the thermal conditions of the envelope, from one to three days or more (when consecutive measurements do not differ by more than 10 %) with measurements at thirty-minute intervals, which implies the observation of changes in surface temperature over time [34].

Thermography is a widespread method for the calculation of the U-value and the scientific community has performed several experiments based on indoor [55,56] and outdoor measurements [57,58]. For outdoor experiments it is necessary to avoid direct exposure of the envelope to rain, snow and solar radiation before and during the experimentation. The wind speed near the façade should be less than 0.5 m/s, while the free wind speed around the building should be less than 5 m/s [59]. The influence of wind on the measurement of the U-value using this method is taken into account by using a convective heat transfer coefficient in the formulation [60]. An additional very important condition that outdoor thermography has demonstrated is the execution of the experimentation on winter nights (when there is a greater temperature difference between indoors and outdoors) [61].

Compared to other conventional U-value measurement methods, such as the point measurement sensors of the HFM method, the IRT method has advantages in the complete visualization of the envelope, facilitating the identification of thermal bridges to avoid measuring the U-value in non-homogeneous areas [62]. While the HFM method requires measurements over three days, the IRT method is presented as a faster method. According to Tejedor. B et al. the length of both methods could be reduced in southern European climatic conditions and extended in northern European countries where climatic conditions are less regular [63]. In the literature, the duration of the thermographic test and the time intervals in thermal imaging is very variable (from a frequency of minutes [64] to hours [65]). Experiments conducted for two to three hours with infrared captures of the envelope every minute, showed deviations of 1–2 % for single leaf walls and 3–4 % for multi-leaf composite walls compared to the HFM method conducted over three days [64]. Fokaides et al. calculated the U-value of several buildings based on three-hour thermographic inspections with measurements taken every twenty minutes and obtained results which were validated using the HFM method by measuring heat flux and surface temperatures. The results showed a deviation between the values provided by both methods of less than 5 % and were very close to the values obtained by also applying the theoretical methodology and a thermohygrometer, confirming the suitability of IR thermography for U-value measurement [66]. In comparison to the theoretical calculation of the U-value, an outdoor thermographic inspection of a newly constructed, very energy efficient building in a single measurement showed deviations between 1–12 % [67]. However, in the inspection of a traditional masonry wall the results derived from the theoretical approach and infrared thermography were similar [68].

In summary, the theoretical method is a fast and inexpensive method, but it requires essential information about the thickness of the material and its thermal properties. Although this information can be obtained from standards, the thermal properties can be altered by material degradation. HFM requires long measurement campaigns and laboratory testing requires expensive facilities and equipment. The IRT method is fast and reliable, but requires precise climatic conditions and the technique is still under development [24]. According to the literature reviewed, thermography is a method that has advantages over other methods. Furthermore, aerial thermography makes it possible to view parts of the building that are inaccessible on foot, reducing the risk of the operation [69]. It is also possible to carry out quick and easy inspections of multiple areas of the same envelope or different buildings in a short period of time, allowing more measurements to be taken compared to using a thermal camera on foot.

The main limitations of airborne thermography identified in the literature, which may negatively affect the accuracy of the results and conclusions of an energy audit, are attributed to the performance of the IR camera used in flight conditions and the experience of the thermographer [70]. On the one hand, attention must be paid to deviations in surface temperature readings. These deviations decrease with flight time, so as the sensors stabilise with ambient conditions, the accuracy of the results improves. For this reason, it is recommended that the IR camera be kept on prior to testing to allow the microbolometer to stabilise with ambient air temperature. Microbolometer infrared cameras include non-uniformity correction (NUC) which adjusts the deviation of the infrared detector when the scene and environment changes. On the other hand, qualification of the thermographer is essential to correctly interpret the thermal imaging results and to identify sources of error that may affect the accuracy of surface temperature measurements.

2.2. Study area

This study was carried out in a university building, the Faculty of Law (Fig. 1), at El Carmen Campus of the University of Huelva, located in south-western Spain (6°56′24″W, 37°15′58″N). Huelva falls within the CSA climate zone as per the Köppen-Geiger climate classification [71]. The region experiences a typical Subtropical-Mediterranean climate with influences from the Atlantic. Winters are characterized by mild and sunny weather, with minimum temperatures rarely dropping below 5 °C. On the other hand, summers are hot and dry, reaching maximum temperatures of approximately 40 °C in July and August.

This is a building constructed in 2001, following lenient regulations regarding energy efficiency, which embodies the typical construction characteristics of buildings in southern Spain where facades are made of brick walls and a finishing layer without thermal insulation. The Faculty

Fig. 1. Building surveyed, located in the city of Huelva (Spain) (The area studied on the building is marked with a red arrow).

of Law building is comprised of several blocks, each with two floors arranged radially. Its envelope was constructed using traditional building methods: brick masonry finished with ceramic tiles.

The experiment was conducted on the facade of an office located on the top floor, facing north to avoid direct sunlight exposure at any time of the day, both in winter and summer (Fig. 2). Due to the radial arrangement of the building, the outdoor thermographic inspection was conducted in a small triangular courtyard with one side opened to the university campus, reducing the impact of climatic variables such as wind.

The office (Fig. 3), with a surface area of 15 m^2 and two windows in its envelope, is equipped with two air conditioning units for heating and cooling. Both remained active during the whole experimental period and the preceding hours to create the maximum thermal difference with the outside. For quantitative inspections it is necessary to apply active thermography in which an external energy source is used to increase the thermal difference between inside and outside. If the purpose of the inspection is qualitative – to identify and locate thermal bridges – passive thermography is applied in which the thermal behaviour of the envelope is evaluated under normal climatic conditions [72].

2.3. Data acquisition and post-processing of UAV IR imagery

The thermometric and the thermographic methods were carried out simultaneously. The test was conducted over 60 h (two days and three nights) during two seasons of the year: winter (from January 16th to 18th) and summer (from June 15th to 17th) in 2023. The equipment used is summarized in Table 1.

In order to monitor the indoor and outdoor climatic conditions during the experiment, the weather station Froggit HP1000SE Pro model (Froggit^{TM}, Koeln, Germany) was installed. It is a wireless Wi-Fi weather station that allows the measurement of several climate parameters every ten minutes: indoor and outdoor air temperatures, humidity level, wind speed and direction, precipitation, and solar radiation. The outdoor sensors of the weather station were installed on the roof of the building (within 20 m of the office and at a height of 2.5 m above the roof) (Fig. 4a), while the indoor sensors were placed inside the office. The indoor air sensor was placed on a table at a height of 1.30 m and a triple surface thermal probe (Testo^{TM}, Titisee-Neustadt, Germany) was integrated to measure the indoor surface temperature of the envelope. The façade surface temperature sensors were placed on the inside wall, in an area centred between the two windows and at a height of 1.70 m. These sensors were fixed with heat conductive adhesive at a distance of 10–15 cm from each other (Fig. 4b).

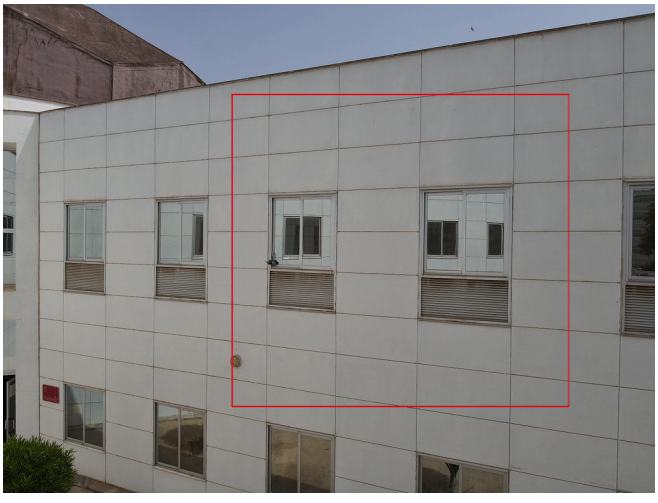

Fig. 2. Building envelope surveyed (The office façade area studied is marked with a red line).

A commercial equipment was used to calculate the U-value (W/m^2K) based on the thermometric method: the Testo 635–2 model (Testo^{TM}, Titisee-Neustadt, Germany). It is a multifunctional tool that calculates the U-value using sensors for measuring indoor wall surface temperature, indoor air temperature and outdoor air temperature. The outdoor air temperature sensor was placed outside an office window and the indoor air temperature and indoor wall surface temperature sensors were placed inside the office next to the above-mentioned triple surface thermal probe and next to a heat flux plate (which was not considered in this experimentation) (Fig. 4b). Using temperature measurements and manually adjusting surface thermal resistances to airflow based on the building envelope's position and heat flow direction [32], this device calculated U-values every ten minutes over the 60-hour experiment in both winter and summer.

In summary, the indoor sensors of both the weather station and the thermometric equipment were located on the façade wall to be analysed and next to it, at a reasonable distance and height and away from the direct influence of the HVAC systems (which are located at ground level). The area of the internal wall where the surface temperature sensors were placed was the area of the wall where the external surface temperatures were measured using airborne thermography.

An UAV equipped with a thermal camera was used to measure the external surface temperatures of the envelope and the reflected temperature of the surroundings recording thermal images of the envelope every hour over a 24-hour period, from the first day to the second night of the test. The equipment used was a DJI Mavic 2 Enterprise Advanced (DJI^{TM}, Nanshan, Shenzhen, China), incorporating a RGB camera for capturing HD images and 4 K video, as well as a radiometric thermal camera capable of extracting temperature data from thermal image pixels. It is a lightweight, foldable multi-rotor UAV with articulated arms, easily transportable and compact, with a take-off weight of 909 g, dimensions of 322x242x84 mm (unfolded), and a maximum flight time of 31 min for battery (three batteries were used in this experimentation and recharged as needed). The RGB camera has a thermal resolution of 48 MP, and the thermal camera has a resolution of 640x512 px. Both cameras operate simultaneously, capturing visual, thermal, or split-view images.

The flight mission was manually planned, paying special attention to the image angle: exact perpendicular between the camera and the object was avoided to minimize potential UAV reflections (especially on materials with low emissivity), and an angle greater than 50° was not exceeded as it could alter the surface temperature readings. Special attention was also paid to the weather conditions to ensure adequate operating conditions for the U-value measurement: rain, snow, severe wind and exposure of the envelope to sunlight were avoided. The weather conditions were optimal, with no rain and a wind speed measured on the roof of the building below 5 m/s: 3.47 m/s in winter and 2.27 m/s in summer.

To ensure accurate measurement of the outdoor surface temperature of the wall, PVC electrical insulating tape was used to calculate the emissivity of the envelope material and a diffuse reflector was used to calculate the reflected temperature during each hourly measurement.

Emissivity describes the ability of an object to emit thermal radiation [73]. Each material has a characteristic emissivity that depends on its composition, colour, texture, and other factors. Emissivity is expressed as a value between 0 and 1, where 0 indicates low emissivity (reflective object) and 1 indicates high emissivity (object that emits all the radiation it should according to its temperature). If the emissivity is low, the apparent temperature will be close to the actual temperature of the objects in the surroundings, while if the emissivity is high, the apparent temperature will be close to the actual temperature of the object. Before conducting the aerial inspection, the emissivity of the building envelope was calculated using the method of PVC electrical tape. In this method, the electrical tape (which has a known emissivity of 0.95) is adhered to the surface of the sample and heated so that the tape and the surface have the same temperature. Then, the surface temperature of the tape is

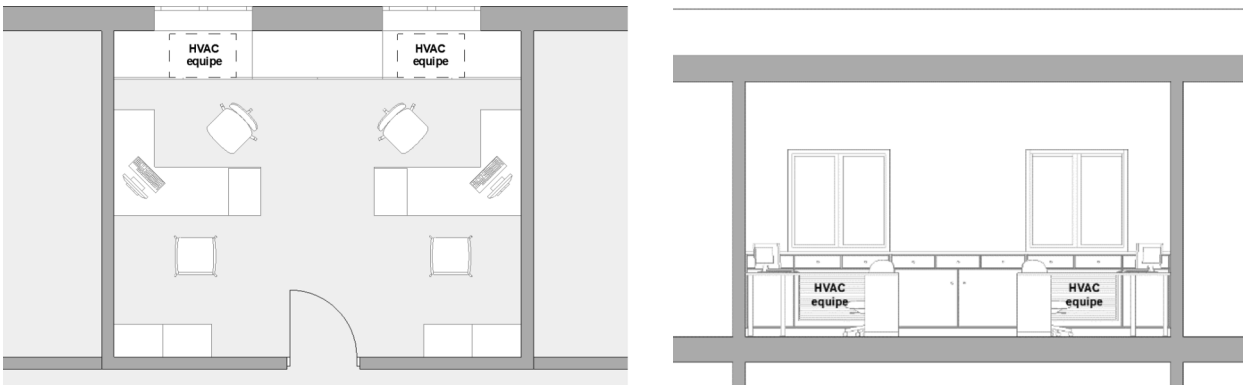

Fig. 3. Plan and interior view of the office.

measured, compared with the surface temperature of the material, and both values are adjusted to obtain the actual emissivity value of the material.

Reflected temperature is the apparent temperature of the surroundings that is reflected by the target in the IR camera [73]. Reflected temperature can significantly influence temperature measurements, especially on objects with low emissivity. During the aerial inspection, while thermal images of the envelope were taken every hour, the reflected temperature of the surroundings was also measured using the reflector method defined in the international standard ISO 18434–1 [74]. In this method, a material with high reflectivity, a diffuse reflector (such as aluminium foil), is used, which is attached to the surface of the facade. Assuming an emissivity of 1 and a distance of 0 in the thermal camera, the temperature measured on the reflective surface is the reflected temperature of the surroundings (Fig. 5).

In thermography, emissivity, reflected temperature from the surroundings, and distance to the object are crucial factors that directly affect the accuracy of infrared temperature measurements and must be measured on-site during experimentation. Distance between the camera and the object is also relevant to compensate for the effect of the atmosphere that absorbs part of the radiation emitted by the objects. The higher the flight altitude or distance to the object, the greater the error in the measurement. In this study, the distance was minimal as the images were taken within 3 m of the facade.

Once the aerial inspection was completed, the thermal infrared images collected were post-processed to extract outdoor surface temperatures and reflected temperatures per hour using DJI Thermal Analysis Tool v.3 software. A set of 48 thermal images were post-processed, 24 images in winter and 24 images in summer (Fig. 6). The average thermal range – indicating the apparent temperature range that can be measured in the IR image – was between 7.0–16.8 °C in the winter images and 25.5–45.7 °C in the summer images. In the post-processing procedure, measured values of emissivity, reflected temperature, and distance were inputted for each thermal image. The outdoor surface temperature was measured in the same area of the envelope where the surface temperature sensors were installed indoors (in a square area of 30x30 cm at a height of 1.70 m between windows, with a homogeneous distribution of surface temperatures and away from the impact of air-conditioning equipment, thermal bridges in the structure and windows). In the DJI Thermal Analysis Tool software, the area measurement tool (Fig. 7) was chosen which provides an average numerical value of the outside surface temperature and was used together with the point average value of the inside surface temperature sensors to calculate the U-value.

2.4. Calculation of thermal transmittance (U-Value)

In the building industry, U-value is the heat transfer per unit area through the building envelope when there is a temperature difference between the indoor and outdoor air. Assuming stationary heat flow and conditions, the U-value is the heat flux per unit area, q, divided by the temperature difference between the two environments that the envelope separates: *Tin* and *Tout* as the indoor and outdoor air temperature, respectively.

$$Uvalue = \frac{q}{Tin - Tout} \tag{1}$$

q is always flowing from the hottest temperature to the coldest. in winter (when $Tin > Tout$) the direction of heat flow is outwards. To avoid negative U-values in summer (when $Tout > Tin$, and the heat flux is inwards), the absolute value of the temperature difference $|Tin\text{-}Tout|$ is considered to allow bidirectional measurements of the heat flux in both seasons.

Depending on the thermal transmittance measurement methodology used, the U-value of a building envelope can be formulated in different ways. According to the thermometric method (Fig. 8), the U-value can be calculated from the temperatures of the envelope and its surroundings. Andújar et al. [52] proposed a framework for quantifying the U-value based on measurements of the surface temperature of the envelope (a façade wall) and the spaces it separates, applying the following equation derived from Newton's law of cooling:

$$Uvalue = \frac{hc(Tin - Ts,in)}{Tin - Tout}\left[\frac{W}{m^2K}\right] \tag{2}$$

where *Tin* (K) is the indoor air temperature, *Ts,in* (K) is the indoor wall temperature, *Tout* (K) is the outdoor air temperature and *hc* is the convection coefficient. Commercial systems that calculate the U-value according to the thermometric method, as the equipment used in this research, apply the equation (2) and the convection coefficient provided in ISO 6946 [32]. The convection coefficient is calculated as the inverse of the surface thermal resistance (*Rsi*) set at 0.13 m^2K/W for vertical enclosures with horizontal heat flow:

$$Rsi = \frac{1}{hc} \tag{3}$$

For the application of thermography in U-value quantification, several methods have been proposed by the scientific community. In indoor thermography, Madding et al. [75] proposed a numerical approach to assess the heat balance in the building envelope using the following equation:

$$Uvalue = \frac{4\varepsilon\sigma Tm^3(Ts,in - Tref) + hc(Ts,in - Tin)}{Tin - Tout}; Tm = \frac{Ts,in + Tref}{2} \tag{4}$$

where ε is the emissivity of the façade, σ is the Stefan-Boltzmann constant, *Ts,in* is the surface temperature of the indoor envelope, *Tref* is the reflected temperature, *hc* is the convection coefficient, *Tin* is the indoor air temperature and *Tout* is the outside air temperature.

Table 1
Material specifications.

Material	Model	Specifications
Weather station 	Froggit HP1000SE Pro model	Transmission frequency: 868 Mhz Transmission range: 100 mOutdoor temperature (°C) : −40 °C to + 60 °CRelative humidity measurement (%) : 10 to 99 %. Rainfall measurement: 0 to 9999 mm Wind speed measurement range: 0–50 m/sIndoor temperature (°C) : −10 °C to + 60 °C
Multifunctional tool 	Testo 635–2 model	Weight: 428 g Dimensions: 220 x 74 x 46 mm Operating temperature: −20 up to + 50 °C Autonomy: 200 h Accuracy: +/- 0.2 °C (between −25 °C to + 74.6 °C) Range: −40 to + 150 °C
UAV 	DJI Mavic 2 Enterprise Advanced	Takeoff Weight (without accessories): 909 g Dimensions: 322 x 242 x 84 mm (unfolded) Max speed: 72 km/h Max flight time: 31 min Spectral band: 8–14 μm Thermal sensor resolution: 640 x 512 pixels Measuring range: −40 °C ~ 550 °C Digital zoom: 32x digital zoom, 16x thermal zoom
DJI Software 	DJI Thermal Analysis Tool	V3.3.0

In outdoor thermography, Dall'O' et al. [60] applied infrared thermography to estimate the thermal transmittance of the envelope using a different heat balance approach. It was assumed that the convective heat exchange with the outside air is equivalent to the heat transfer through the wall:

$$Uvalue = \frac{hc\,(Ts,out - Tout)}{Tin - Tout};\ hc = 5.8 + 3.8054v \tag{5}$$

where *Ts,out* represents the surface temperature of the outer wall, *Tout* is the outdoor air temperature, *Tin* is the indoor air temperature and *hc* is the convection coefficient, which is calculated as a function of the wind speed, *v*, according to the Jürges' equation [76].

Albatici et al. [59] extended the work in the field of thermography for the evaluation of thermal transmittance using the heat balance ratio for the exterior of a wall by means of the following equation:

$$Uvalue = \frac{\varepsilon\sigma\left(Ts,out^4 - Tout^4\right) + 3.8054v(Ts,out - Tout)}{Tin - Tout} \tag{6}$$

where ε is the emissivity of the façade, σ is the Stefan-Boltzmann constant, *Ts,out* is the outside surface temperature of the envelope, *Tout* is the outside air temperature, *Tin* is the indoor air temperature and *v* is the wind speed.

Based on the outdoor thermography (Fig. 9), this study used the equation proposed by Bayomi et al. [29], which incorporates aerial infrared data to calculate the U-value:

$$Uvalue = \frac{\varepsilon\sigma(Tref - Ts,in) + hc(Tin - Ts,in)}{(Ts,in - Ts,out)}\left[\frac{W}{m^2K}\right] \tag{7}$$

where ε is the emissivity of the façade, σ is the Stefan-Boltzmann constant ($5.67x10^{-8}$ W/m^2K^4), *Tref* (K) is the reflected temperature, *Ts,in* (K) is the indoor wall temperature, *Tin* (K) is the indoor air temperature, *Ts, out* (K) is the outdoor wall temperature and *hc* is the convection coefficient set at 8.7 $W/(m^2K)$ by the authors of the above-mentioned research. In this study, the emissivity value was calculated at 0.95 using the PVC electrical tape method.

Based on different studies, the convective heat transfer coefficient has a significant influence on the results [60]. The large variability of convection coefficient calculation approaches proposed by the scientific community (mainly formulations correlated with wind speed and dimensionless numbers) were identified in the literature and compared, but no single valid coefficient could be standardised [77].

2.5. Validation of U-value

To validate the accuracy of aerial thermography as an U-value calculation method, the U-value measured with the thermometric method were compared with the U-value calculated using the thermal information recorded with the UAV. For this purpose, two statistical metrics were used: coefficient of determination (R^2) and root mean square error (RMSE).

The statistical index R^2, also known as the coefficient of determination, is a measure used in linear regression and other regression models to assess the goodness of fitting the model to the observed data. In other words, it is a measure of the goodness-of-fit or reliability of the estimated model to the reference data. The statistical index RMSE (Root Mean Squared Error) is a commonly used measure to assess the accuracy of a regression or prediction model. It is calculated as the square root of the average of the squared errors between the observed values and the values predicted by the model. RMSE measures the average difference between the actual values and the values predicted by the model [78].

$$\mathrm{RMSE} = \sqrt{\sum_{i=1}^{N}\frac{(Predictedi - Actuali)^2}{N}} \tag{8}$$

3. Results

According to the previously described methodology, the research results are presented below. The first section analyses U-values measured with the thermometric method for 60 h in both winter and summer. The second section shows the calculated U-value data following the thermographic methodology for a typical winter day and a typical summer day. Finally, in the third section, the U-value results are compared using statistical metrics.

3.1. U-values according to the thermometric method

The results of the U-values obtained from thermometric measurements during 60 h in winter and summer are presented below. The experiment was carried out over three nights and two days.

a) b)

Fig. 4. Equipment: a) Weather station located in the roof of the building, b) Indoor air and wall surface temperature sensors placed on the surveyed façade.

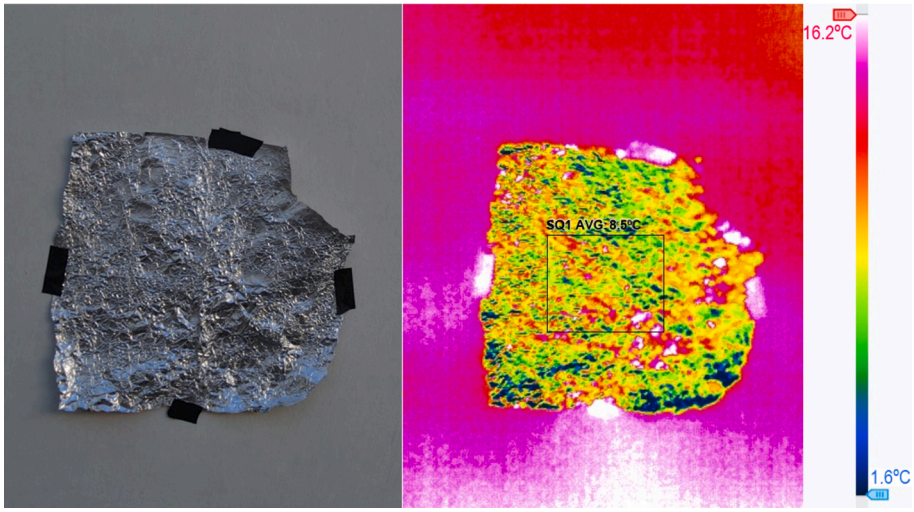

Fig. 5. Example of reflected temperature measurement.

Fig. 10 illustrates temperature values (outside, inside, and indoor wall surface) along with the corresponding U-values measured for three winter days (16–18 January 2023). In terms of the length of the day during winter, the sun rises at 08:40 a.m. and sets at 18:33p.m., providing 9 h and 52 min of daylight and 14 h and 7 min of nighttime.

Throughout the experiment, the indoor temperature of the building remained consistently stable, averaging 28.3 °C. No significant differences were observed between day and night temperatures. However, the indoor wall surface temperature was slightly lower than the indoor air temperature, averaging 25.9 °C. Outdoor temperatures exhibited notable variations between days, with the first day being warmer at 15.6 °C, compared to 12.6 °C on the second day. Nighttime outside temperatures ranged between 12.5 °C on the first night, 11.4 °C on the second night, and 8.2 °C on the last night.

Concerning the thermal transmittance of the building envelope, stable U-values were measured during the nights, when the greatest temperature difference between the indoor and outdoor environments was recorded. Consistent values of around 1.0 W/m^{2}K were observed throughout the experimental nights. U-values exhibited variability during the daytime hours of the experiment, with a mean ranging between 1.5 and 1.7 W/m^{2}K. At 15:00 h, when the minimum thermal difference between indoors and outdoors was recorded, maximum values of 3.0 W/m^{2}K were reached on the first day, and 2.2 W/m^{2}K on the second day.

Fig. 11 shows the temperatures and U-values recorded for three summer days (15–17 June 2023). In the summer period, the duration of daylight and nighttime hours is as follows: sunrise at 07:06 a.m. and sunset at 21:49p.m., resulting in 14 h and 43 min of daylight and 9 h and 17 min of nighttime.

In terms of temperature, the indoor temperature within the building remained consistently stable throughout both days and nights during the experiment, averaging 20.5 °C. The inner wall surface temperature showed a similar thermal pattern to the indoor temperature but slightly higher, with an average of 22.5 °C. Outdoor temperatures barely varied between days, averaging 28.7 °C on the first day and 29.4 °C on the second day. The average outdoor temperature remained relatively

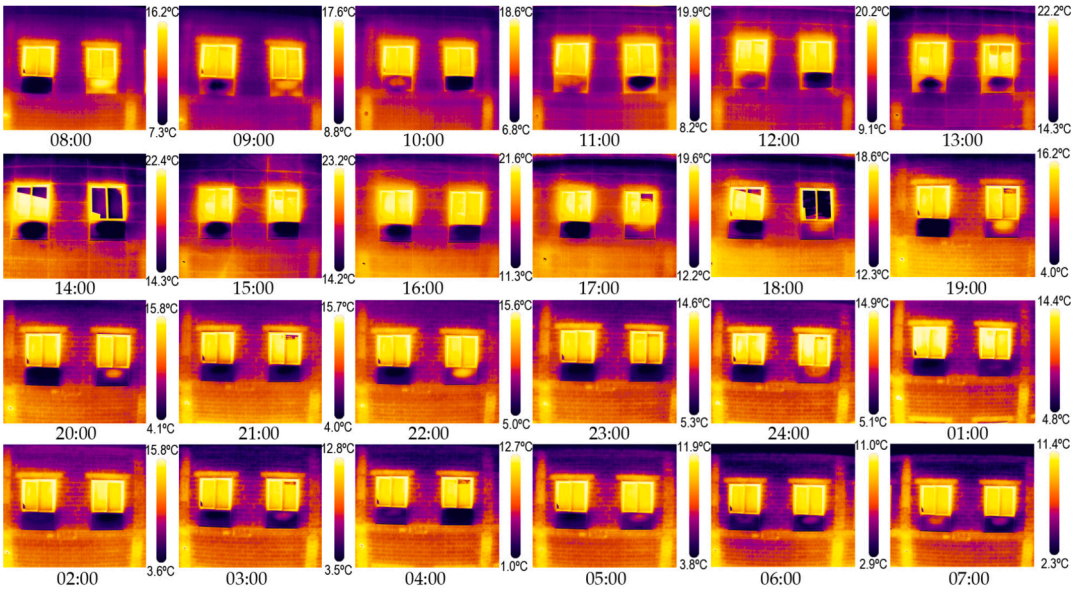

a)

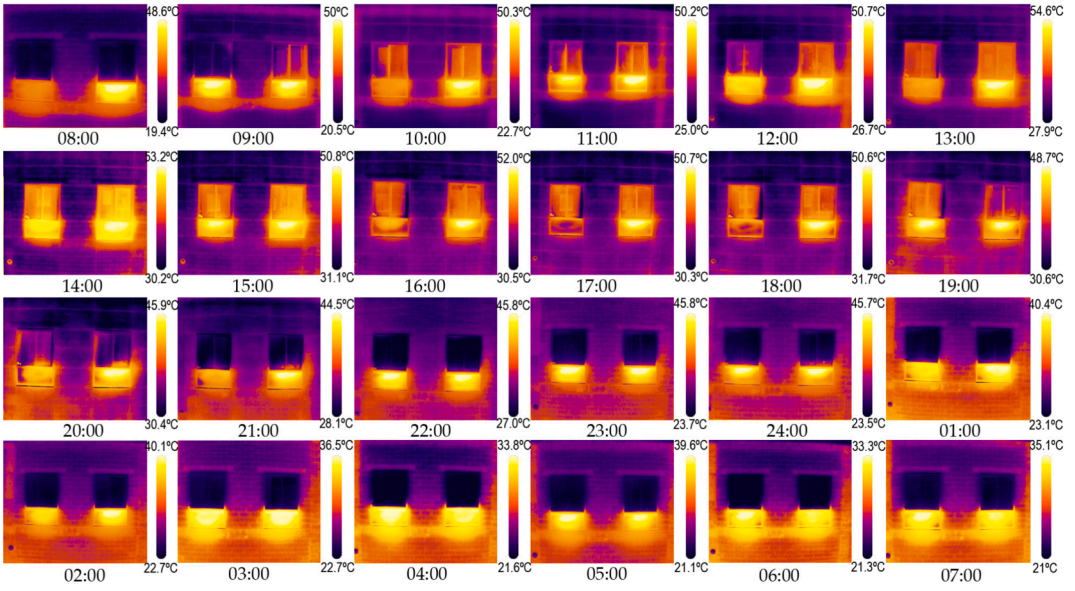

b)

Fig. 6. IR Images of the building envelope over 24 h in: a) winter, b) summer.

consistent over the three nights of the experiment, averaging 23.7 °C.

Regarding the thermal transmittance of the building envelope, it was observed that the measurements exhibited significant irregularity between days and nights. During the night, the U-values reached maximum peaks ranging between 7.7 and 12.1 W/m^{2}K when the minimum thermal difference between indoors and outdoors was recorded. The outdoor temperatures reached their lowest value and matched indoor temperatures in the pre-dawn hours. During the daytime, mean U-values between 1.8 and 2.2 W/m^{2}K were measured. Minimum values ranging from 1.2 to 1.4 W/m^{2}K were recorded when the greatest temperature difference between indoors and outdoors occurred at midday.

3.2. U-values according to the thermographic method

The results of the U-values calculated using the thermographic methodology during a typical winter day and a typical summer day are presented below. The experiment was carried out on the first day and the second night of the three full days of the experiment.

Fig. 12 displays the measured temperature values and the calculated U-values during a typical winter day (17 January 2023). The U-values measured with the thermometric method in the previous section are also plotted graphically and are referred to as reference data. On a typical winter day, the average measured temperatures were 27.9 °C inside, 25.8 °C on the indoor wall surface, 15.6 °C outside during the daytime, and 11.4 °C outside at night.

The outdoor wall surface temperature was higher than the outside air temperature, averaging 16.4 °C during the day and 13.4 °C at night. The difference between both temperatures was greatest during the night. During the main hours of the day, the outdoor wall surface temperature matched the outside air temperature.

The calculated U-values exhibited the same trend as the reference U-values. During the typical winter night (from 18:33p.m. to 08:40 a.m.),

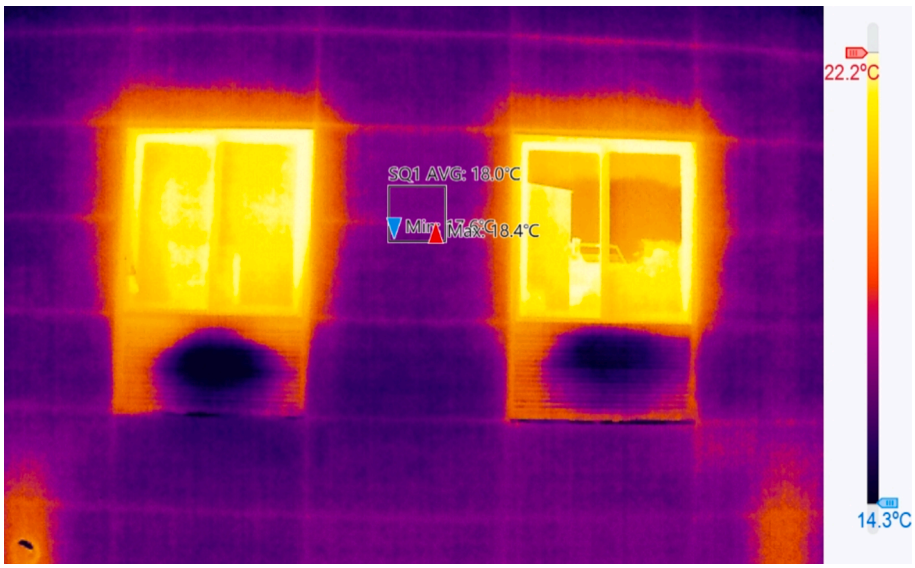

Fig. 7. Example of outdoor surface temperature measurement.

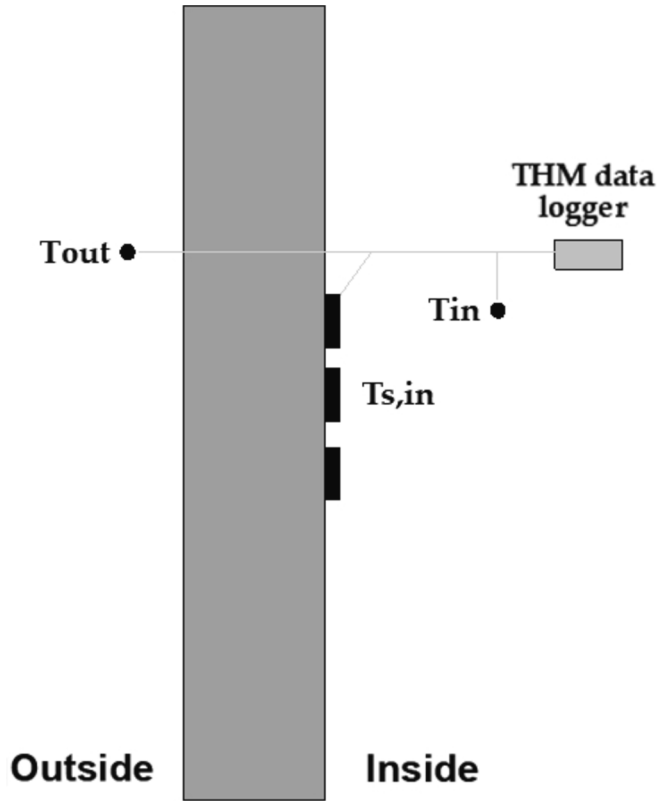

Fig. 8. Schematic diagram of thermometric method.

the mean of the calculated U-values was 1.0 W/m^{2}K, matching the reference values. There was also agreement between the values obtained in the early morning hours until 12:00 h. However, in the midday hours, U-values were slightly overestimated by an average of + 0.5 W/m^{2}K compared to the reference values, reaching the maximum peak at 15:00 h (3.5 W/m^{2}K).

Fig. 13 displays the measured temperature values, the calculated U-values, and the reference U-values (the thermometric values) during a typical summer day (16 June 2023). The average measured inside temperature was 20.3 °C, the indoor wall surface temperature was

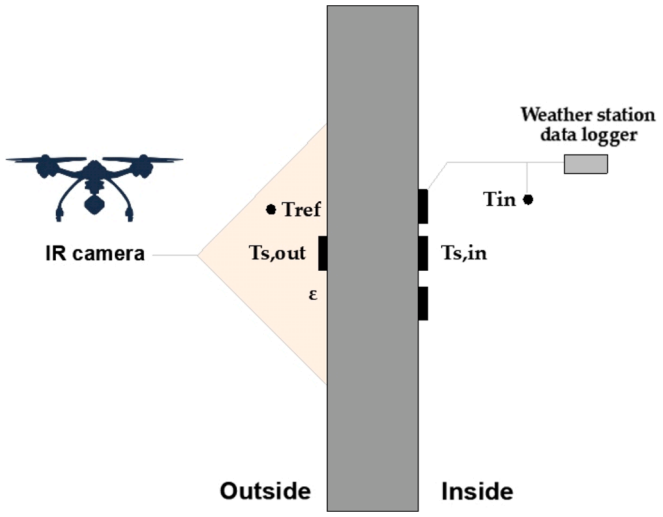

Fig. 9. Schematic diagram of outdoor aerial thermography.

22.4 °C, the outside daytime temperature was 28.7 °C, and the outside nighttime temperature was 23.7 °C.

As in winter, the outdoor wall surface temperature was higher during the night hours, while during the daytime, it was closer to the outdoor air temperature. The outdoor wall surface temperature recorded an average of 29.5 °C during the day and 25.6 °C at night.

Regarding the calculation of the U-values, it exhibited a trend similar to the reference data due to significant differences observed between night and day measurements. During the night, in the pre-dawn hours when indoor and outdoor temperatures matched, the calculated U-values showed both overestimations and underestimations with respect to the reference data in a short period of time. Unstable values were obtained, reaching maximum peaks of 7.0 W/m^{2}K. Throughout the day and early evening, it was observed that the calculated U-values were over scaled compared to the reference data by an average of + 1.0 W/m^{2}K. The minimum U-values (1.9 W/m^{2}K) were obtained during the daytime hours, as in the reference data, but were higher with a difference of + 0.7 W/m^{2}K.

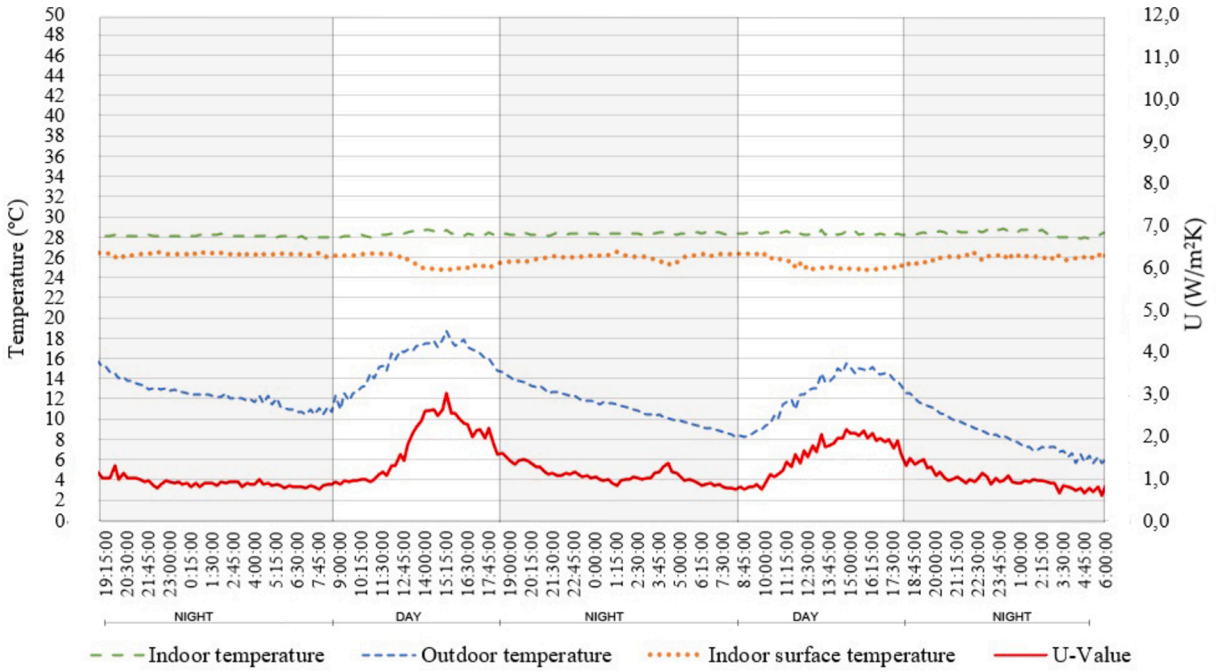

Fig. 10. U-Values measured according to the thermometric method on winter days.

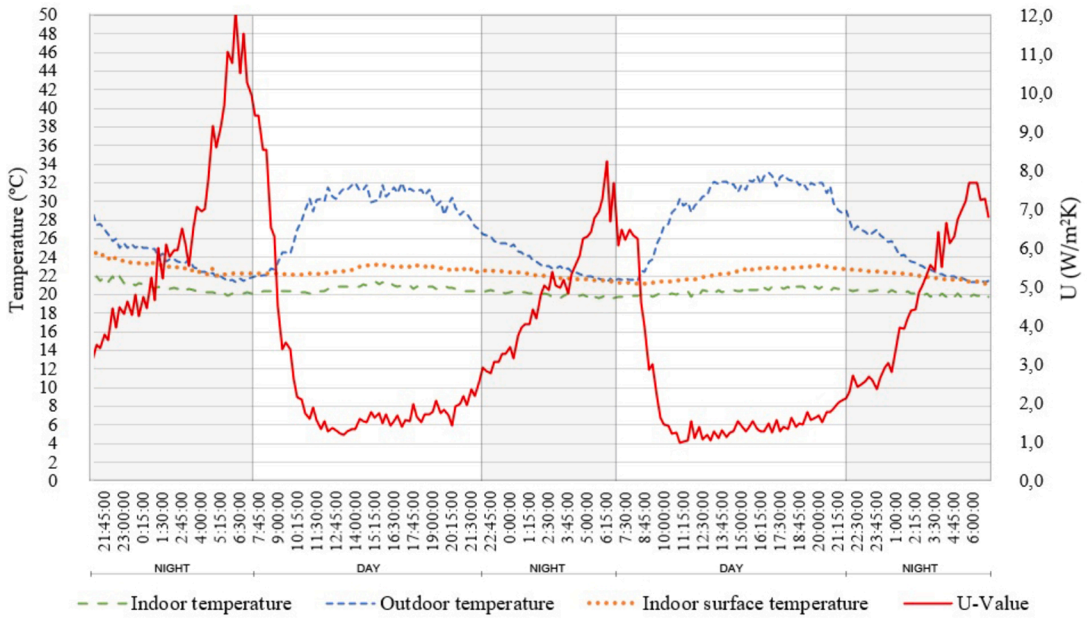

Fig. 11. U-Values measured according to the thermometric method on summer days.

3.3. Comparison and validation of U-values

Fig. 14 illustrates the linear relationship between the U-values measured with the thermometric method and the thermographic method on a typical winter day (Fig. 11a) and a typical summer day (Fig. 11b). The results demonstrate a strong coefficient of determination (R^2) across all analysed points, totalling 184 samples in each scenario. The R^2 is 0.978 for a typical winter day and 0.902 for a typical summer day. A high R^2, close to 1, indicates that the estimated model fits well with the baseline data. However, it is important to note that while R^2 analyses the trend of the data, it does not solely determine the quality of the model.

For this reason, another index was considered: the root mean square error (RMSE), which quantifies the error between the two databases. The lower the RMSE value, the better the predictive capability of the model. The RMSE revealed differences between the thermometric and the thermographic values during the typical summer day. In this scenario, the RMSE was 0.96 W/m^{2}K during the day and 0.85 W/m^{2}K at night, representing a considerable error of 29.1 % and 25.8 %, respectively, compared to the mean of all data analyzed in summer (3.28 W/m^{2}K). However, the RMSE was better during the typical winter day, especially at night. The RMSE was 0.35 W/m^{2}K during the day and 0.06 W/m^{2}K at night, representing an error of 25.0 % and 4.3 %, respectively, in relation to the mean of the data analyzed in winter (1.36 W/m^{2}K).

Since more accurate results were obtained on the typical winter night, an uncertainty analysis of the U-value was performed using the

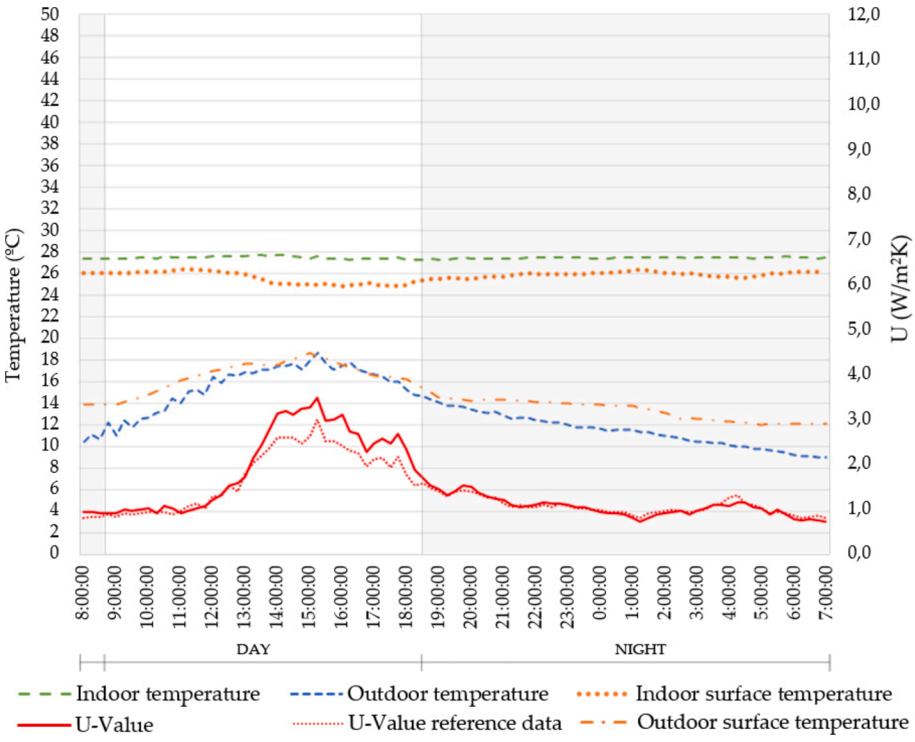

Fig. 12. U-Values calculated according to the thermographic method on a typical winter day.

average of the temperatures measured with both methods. For this purpose, a Monte Carlo simulation was carried out using Matlab R2020a software (The MathWorks Inc., Natick, Massachusetts, USA). The objective of a Monte Carlo simulation is to approximate the probability distribution of the output (U-values) from the uncertainty of the input variables associated with the equipment used.

Monte Carlo simulation generates random numbers in the uncertainty ranges of the input data assuming a uniform or Gaussian distribution. By randomly sampling each of the inputs and perturbing them simultaneously, it is possible to estimate a potential output result and its standard deviation using a probability distribution function. To achieve this, it is necessary to run enough simulations (in this case $N = 10^6$) to obtain a correct estimate of the mean, standard deviation and confidence interval. In addition to the probability distribution of the U-values, sensitivity coefficients were calculated that measure how the uncertainty of an input variable affects the uncertainty in the model output (Table 2). Fig. 15 shows the probability distribution of the U-values obtained by performing the Monte Carlo simulation with both methods.

The results of both simulations showed an average U-value of 1.039 W/m^{2}K for the thermometric method and 1.011 W/m^{2}K for the thermographic method. Regarding the standard deviation and confidence intervals, on the one hand, the thermometric method provided an uncertainty of ± 0.037 W/m^{2}K which gives a confidence interval of 68.3 % between 1.002 and 1.076 W/m^{2}K and a confidence interval of 95.5 % between 0.966 and 1.112 W/m^{2}K and, on the other hand, the thermographic method provided an uncertainty of ± 0.121 W/m^{2}K giving a confidence interval of 68.3 % between 0.890 and 1.132 W/m^{2}K and a confidence interval of 95.5 % between 0.779 and 1.257 W/m^{2}K.

4. Discussion

Analysing the results obtained from the experimentation conducted over three typical winter days and three typical summer days using the thermometric method, it was found that U-values are highly variable and are greatly influenced by the thermal difference between the two spaces separated by the envelope and by changes in outdoor temperatures.

After the six full days of experimentation in both seasons, there was only a lengthy period during which a stable U-value was measured: winter nights. During this time frame, constant U-values of 1.0 W/m^{2}K were measured over the three nights of winter experimentation. The thermal difference between indoors and outdoors was crucial, as stable U-values were measured when the maximum thermal difference in winter was recorded: a difference of 15.8 °C on the first night, 16.9 °C on the second night, and 20.1 °C on the third night.

The significance of thermal amplitude was also evident during summer nights when outdoor and indoor temperatures matched – the thermal difference was 0 °C – and unstable and distorted U-values were measured, reaching peaks of up to 12.1 W/m^{2}K. In both winter and summer, maximum U-values were measured when the lowest thermal difference between indoors and outdoors was observed, while minimum U-values were measured when the highest thermal difference between indoors and outdoors was recorded. Regardless of the method, to calculate the U-value it is essential to ensure large thermal differences on both sides of the wall. As in this case, external energy sources are normally used to heat or cool the interior space. Research in Mediterranean climates has shown that U-values are overestimated when temperature differences between inside and outside are minimal (deviations of 150 % with thermal differences between 3–4 °C, 100 % with differences between 4–5 °C and 60 % with differences of 6 °C) [56].

However, in addition to thermal difference, it is also crucial that U-value measurements are stable and constant over long periods of time for an accurate assessment. In both summer and winter days, despite measuring thermal amplitudes around 10 °C (8.6 °C in summer and 14.2 °C in winter), stable and constant values were not recorded over an extended period. During summer days, the average U-value was 2.0 W/m^{2}K, reaching minimums of up to 1.2 W/m^{2}K, while in winter days, the average U-value was 1.6 W/m^{2}K, reaching maximums of up to 3.0 W/m^{2}K. During the daytime experimentation in both periods, instability was observed between outdoor temperature measurements over short periods of time which may be caused by cloud movement, shading and

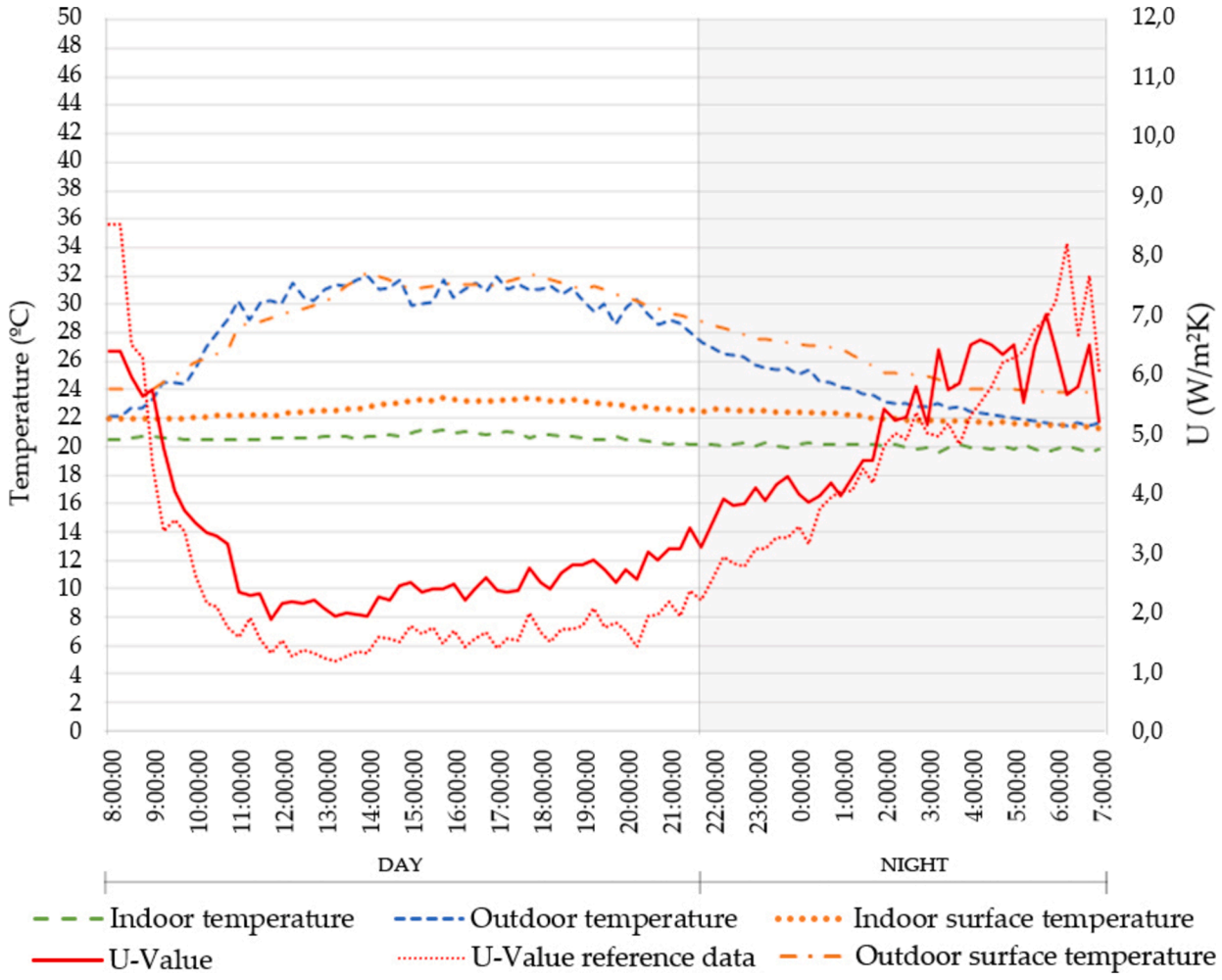

Fig. 13. U-Values calculated according to the thermographic method on a typical summer day.

light effects on the environment and air masses.

Furthermore, in summer, the indoor surface temperature was slightly higher during the day than at night. In winter, however, it was slightly lower during the day. This indicates that the indoor surface temperature increases as the thermal difference between indoors and outdoors becomes greater, in both seasons.

On the comparison between U-values calculated using thermometric and thermographic methods in a 24-hour cycle in winter and summer, the models demonstrated a high coefficient of determination (R^2 of 0.978 in winter and 0.902 in summer), indicating that the thermographic method provided results that follow the same trend as the data measured with the thermometric method. However, the RMSE index quantified a considerable error in some periods of the day and the year. On one hand, stable results (U-value = 1.0 W/m^{2}K) were obtained during the night and early morning hours of winter. Between methods, it was measured a minimal difference of 0.06 W/m^{2}K which represents an error of 4.3 %. On the other hand, overestimated U-values were obtained, 0.35 – 0.96 W/m^{2}K higher during the winter day and the summer day respectively, although the façade was not directly exposed to the sun. This represents a considerable error (between 25.0—29.1 %) given the low magnitude of the reference data. The main challenge of conducting this experimentation during daylight hours, regardless of the method used, lies in the rapid fluctuations in temperature.

In other research, it has been shown that direct solar exposure of the wall has a great influence on the accuracy of the measurement, especially in the late afternoon, due to the heat stored in the wall [59]. It is important to avoid measurement if the surveyed wall is exposed to direct solar irradiation for a long time, as transient thermal phenomena can lead to measurement errors. On a winter day, considerable differences between 1–48 % were obtained by comparing the U-values obtained with thermography and HFM of a non-north facing façade subjected to solar exposure [79]. Like in this case, even if the test is carried out under winter conditions and direct solar incidence is avoided during the day, the U-values calculated with thermography during daylight hours have also shown some uncertainty (between 2 and 37 %) when compared to other methods such as HFM [67].

Additionally, during summer nights, U-values were calculated with a high associated error (25.8 %). It is essential to mention that during that time frame, the reference U-values measured were also highly variable and reached disproportionate values due to the non-existent thermal difference between the interior and exterior of the building – an uncertainty that was reflected in the results measured with both methods. As in other research where the THM method was applied in summer in a Mediterranean climate and U-values with differences of around 20 % were obtained, the uncertainty associated with testing at this time of year is unacceptable [48]. The main limitation of this study is the significant difference between U-values measured in winter and summer. It is not advisable to calculate summer U-values using aerial thermography, as has been shown by other authors using conventional methods [43].

The fact that both methods yield similar results, especially during winter nights, suggests that both models are more reliable under these temperature conditions (more stable over time and with greater thermal amplitude). However, due to discrepancies in the U-value results

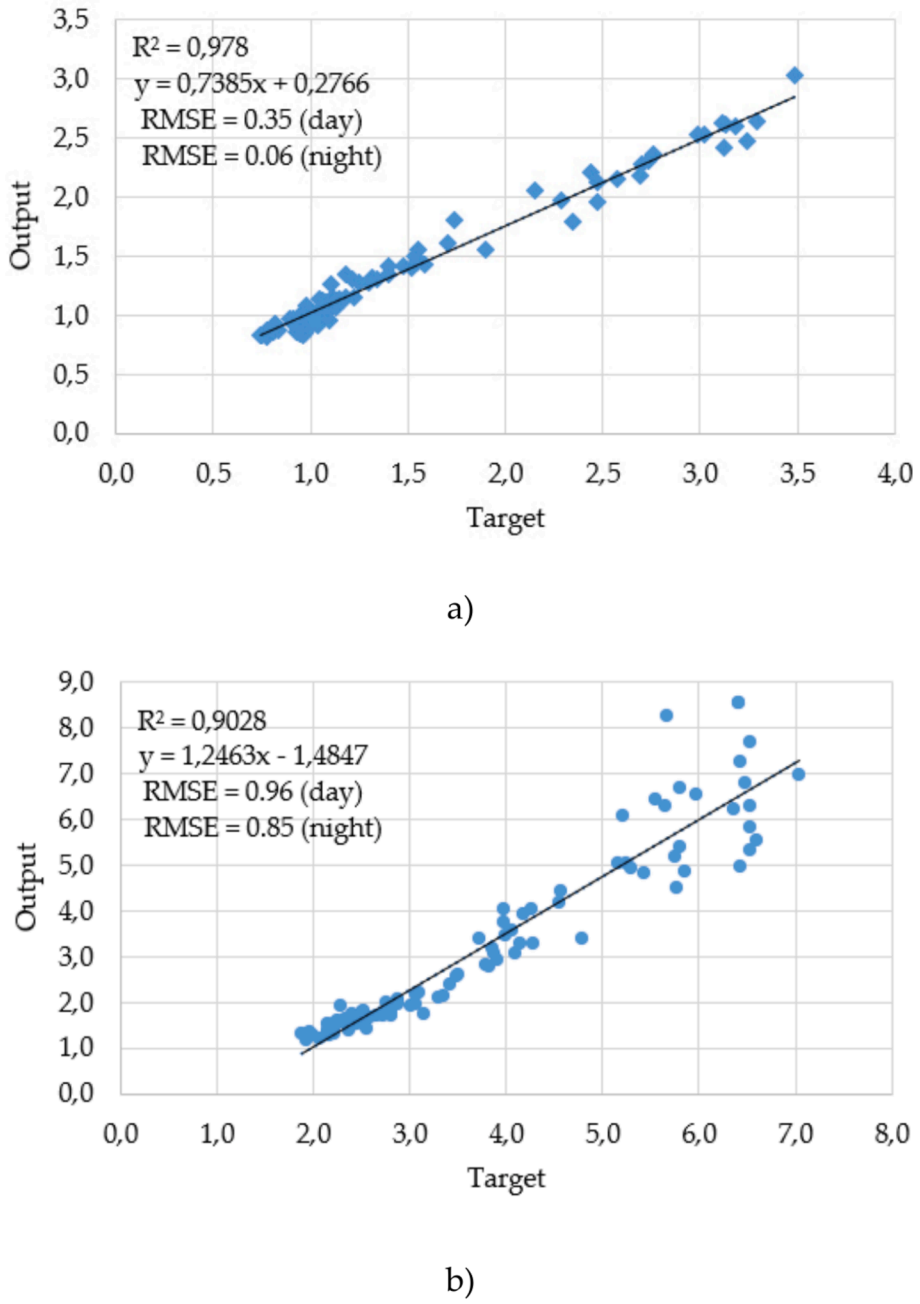

Fig. 14. Comparison of U-values measured with the thermometric and the thermographic methods (R^2 and RMSE): a) on a typical winter day, b) on a typical summer day.

Table 2
Input variables with standard deviation u (x_i) and sensitivity coefficients u (c_i).

Thermometric method				Thermographic method			
Input variable	u(xi)	Distribution	c(xi)	Input variable	u(xi)	Distribution	c(xi)
Tin	±0.2 K	Gaussian	0.5536	Tin	±0.5 K	Gaussian	0.7629
Ts,in	±0.2 K	Gaussian	0.5568	Ts,in	±0.2 K	Gaussian	1.8229
Tout	±0.3 K	Gaussian	0.3746	Tref	±2.0 K	Gaussian	0.1831
				Ts,out	±2.0 K	Gaussian	0.1831

throughout the whole experiment, an uncertainty analysis was conducted to interpret the differences between the two mathematical models. While the thermometric model showed a standard deviation of ± 0.037 W/m^{2}K, the thermographic model exhibited a standard deviation of ± 0.121 W/m^{2}K. The results of the uncertainty analysis and sensitivity coefficients, which demonstrate how uncertainty is amplified in the input variables of the mathematical model used in the thermographic method, highlight the importance of using high-precision temperature measurement equipment to minimize uncertainty in the U-value output.

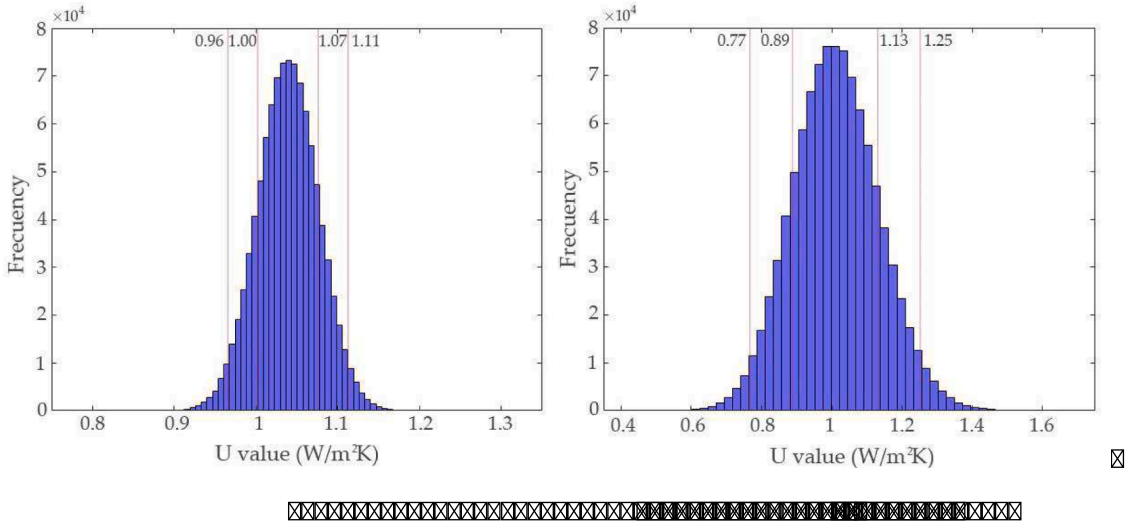

Fig. 15. Comparison of the probability distribution of the simulated U-values: a) with the thermometric method, b) with the thermographic method.

Based on the results obtained and the limitations identified, it is recommended for future work to use aerial thermography exclusively during winter nights when there is maximum thermal amplitude (more than 15 °C) and temperatures are more stable. Additionally, it is suggested to increase the frequency of measurements (every 10–15 min), to repeat the aerial experimentation over several nights during the same time period (which can be reduced to the post-midnight and pre-dawn hours) and to use highly accurate temperature sensors with the lowest associated error to prevent it from propagating through the model and affecting the output value.

If mechanical equipment is used to amplify the thermal difference between indoors and outdoors, it is recommended to consider that HVAC systems can disturb the measurements, so it is recommended not to place sensors close to their airflow and not to take measurements of the outside surface temperature in the surroundings of the equipment if it is installed on the wall to be inspected. It is also not recommended to take surface temperature measurements in areas where the temperature distribution is not homogeneous, such as thermal bridges. If the purpose is to calculate the U-value of the complete building envelope, it is advisable to perform the calculation on each of the building façades and obtain an average U-value, as this value may differ slightly depending on the façade orientation even if the composition and thicknesses of the materials are similar. Kim et al. applied the HFM and THM methods to estimate the U-value of several buildings and showed an average difference of 0.13 W/m^{2}K between the U-values of north, south, east and west facing facades of the same building [53]. Evangelisti et al. calculated a difference of 0.14 W/m^{2}K between the U-values of two north- and south-facing facades of the same building in winter [44].

5. Conclusion

The measurement of the U-value is essential in the field of building energy renovation. The purpose of this research is to evaluate aerial thermography, applying unmanned aerial vehicles (UAVs) equipped with infrared (IR) thermal cameras, to overcome common physical limitations in traditional building auditing methods. This approach is particularly beneficial when assessing large buildings or building complexes.

In this research, the calculation of thermal transmittance (U-value) has been addressed by two methodologies based on temperature measurements, the thermometric and the aerial thermographic methods. Based on the results obtained in this research and supported by findings from the scientific community, the use of aerial thermography is considered valid as a method to estimate the U-value in subtropical mediterranean climates, provided it is conducted under winter nocturnal conditions ensuring a minimum thermal amplitude above 15 °C. It is suggested that the application of airborne thermography be carried out continuously over several nights (in post-midnight and pre-dawn hours), taking measurements every 10 to 15 min and using high accuracy temperature sensors to minimise errors in the model, in order to establish a preliminary U-value that can be used in the initial stages of a building energy audit.

After analysing the calculation of the U-value during the winter and summer days and nights, it is determined that the winter night was the only period in which stable and constant U-values (1 W/m^{2}K) were obtained using both methods. In addition, this was the period of the year when the highest indoor/outdoor temperature difference (about 16.9 °C) was measured. However, a large thermal difference is not the only condition necessary for a correct U-value measurement, as summer climatic conditions and rapid temperature fluctuations during the day have been shown to generate greater variations in the U-value. The viability of experimentation during summer days and nights, as well as winter days, is disregarded even if it is carried out on a north-facing façade without direct solar incidence. It is necessary that U-value measurements are stable and constant over long periods of time for an accurate assessment. For this reason, this methodology cannot be simplified to a single measurement.

The proposed framework addresses various challenges present in current energy auditing processes for buildings, such as the difficulty of physical access to components like high roofs or facades, which are often challenging to inspect using conventional methods. The results obtained are expected to provide a baseline to facilitate the applicability of the method to other buildings. Furthermore, this framework presents significative advantages at the neighbourhood level to analyse and determine the most efficient adaptation strategies, as well as to identify time savings and cost reductions achievable by evaluating multiple buildings compared to traditional inspection processes.

CRediT authorship contribution statement

Marta Videras Rodríguez: Writing – original draft, Software, Investigation, Data curation, Conceptualization. **Sergio Gómez Melgar:** Writing – review & editing, Validation, Supervision, Methodology, Conceptualization. **José Manuel Andújar Márquez:** Writing – review & editing, Supervision, Funding acquisition.

Declaration of competing interest

The authors declare the following financial interests/personal relationships which may be considered as potential competing interests: Sergio Gomez Melgar reports administrative support and article publishing charges were provided by University of Huelva. If there are other authors, they declare that they have no known competing financial interests or personal relationships that could have appeared to influence the work reported in this paper.

Data availability

Data will be made available on request.

References

[1] Parlamento Europeo y Consejo de la Unión Europea, *Directiva 2012/27/UE del parlamento Europeo y del Consejo de 25 de octubre de 2012 relativa a la eficiencia energética*. 2012, pp. 1–56.

[2] Parlamento Europeo y Consejo de la Unión Europea, *Directiva 2010/31/UE del parlamento Europeo y del Consejo de 19 de mayo de 2010 relativa a la eficiencia energética de los edificios*. 2010, pp. 1–23.

[3] Jefatura del Estado, *Ley 8/2013, de 26 de junio, de rehabilitación, regeneración y renovación urbanas*. 2013, pp. 1–32.

[4] S. Gómez Melgar, M.Á. Martínez Bohórquez, J.M. Andújar Márquez, uhuMEBr: Energy Refurbishment of Existing Buildings in Subtropical Climates to Become Minimum Energy Buildings, Energies 13 (5) (2020) 1204, https://doi.org/10.3390/en13051204.

[5] Z. Ma, P. Cooper, D. Daly, L. Ledo, Existing building retrofits: Methodology and state-of-the-art, Energy Build. 55 (2012) 889–902, https://doi.org/10.1016/j.enbuild.2012.08.018.

[6] B. Nicolae, B. George-Vlad, Life cycle analysis in refurbishment of the buildings as intervention practices in energy saving, Energy Build. 86 (2015) 74–85, https://doi.org/10.1016/j.enbuild.2014.10.021.

[7] M. Khoukhi, A. Hassan, S. Abdelbaqi, The impact of employing insulation with variant thermal conductivity on the thermal performance of buildings in the extremely hot climate, Case Stud Therm. Eng. vol. 16, no. November (2019) 100562, https://doi.org/10.1016/j.csite.2019.100562.

[8] S. Ilomets, K. Kuusk, L. Paap, E. Arumägi, T. Kalamees, Impact of linear thermal bridges on thermal transmittance of renovated apartment buildings, J. Civ. Eng. Manag. 23 (1) (2017) 96–104, https://doi.org/10.3846/13923730.2014.976259.

[9] S.B. Sadineni, S. Madala, R.F. Boehm, Passive building energy savings: A review of building envelope components, Renew. Sustain. Energy Rev. 15 (8) (2011) 3617–3631, https://doi.org/10.1016/j.rser.2011.07.014.

[10] B. Tejedor, E. Barreira, R.M.S.F. Almeida, M. Casals, Thermographic 2D U-value map for quantifying thermal bridges in building façades, Energy Build. 224 (2020) 110176, https://doi.org/10.1016/j.enbuild.2020.110176.

[11] S.L. Wong, K.K.W. Wan, D.H.W. Li, J.C. Lam, Impact of climate change on residential building envelope cooling loads in subtropical climates, Energy Build. 42 (11) (2010) 2098–2103, https://doi.org/10.1016/j.enbuild.2010.06.021.

[12] G. Feng, S. Sha, X. Xu, Analysis of the Building Envelope Influence to Building Energy Consumption in the Cold Regions, Procedia Eng. 146 (2016) 244–250, https://doi.org/10.1016/j.proeng.2016.06.382.

[13] E. C. Shao, Detecting sources of heat loss in residential buildings from infrared imaging, Thesis - Massachusetts Inst. Technol. Dept. Mech. Eng., 2011, [Online]. Available: https://dspace.mit.edu/handle/1721.1/68921.

[14] M. H. Elnabawi, E. Saber, L. Bande, Passive Building Energy Saving: Building Envelope Retrofitting Measures to Reduce Cooling Requirements for a Residential Building in an Arid Climate, *Sustain.*, vol. 16, no. 2, 2024, doi: 10.3390/su16020626.

[15] J. Huang, S. Wang, F. Teng, W. Feng, Thermal performance optimization of envelope in the energy-saving renovation of existing residential buildings, Energy Build. 247 (2021) 111103, https://doi.org/10.1016/j.enbuild.2021.111103.

[16] S. Schiavoni, F. D'Alessandro, F. Bianchi, F. Asdrubali, Insulation materials for the building sector: A review and comparative analysis, Renew. Sustain. Energy Rev. 62 (2016) 988–1011, https://doi.org/10.1016/j.rser.2016.05.045.

[17] Ü. Alev, et al., Renovation alternatives to improve energy performance of historic rural houses in the Baltic Sea region, Energy Build. 77 (2014) 58–66, https://doi.org/10.1016/j.enbuild.2014.03.049.

[18] J. Lee, J. Kim, D. Song, J. Kim, C. Jang, Impact of external insulation and internal thermal density upon energy consumption of buildings in a temperate climate with four distinct seasons, 2016, pp. 1081–1088, Renew. Sustain. Energy Rev. 75 (November) (2017), https://doi.org/10.1016/j.rser.2016.11.087.

[19] Comite Europeen de Normalisation, *EN ISO 9972:2015 Thermal performance of buildings - Determination of air permeability of buildings - Fan pressurization method*. 2015.

[20] E. Kamel, A Systematic Literature Review of Physics-Based Urban Building Energy Modeling (UBEM) Tools, Data Sources, and Challenges for Energy Conservation, Energies 15 (8649) (2022) 24.

[21] F. Asdrubali, G. Baldinelli, F. Bianchi, A quantitative methodology to evaluate thermal bridges in buildings, Appl. Energy 97 (2012) 365–373, https://doi.org/10.1016/j.apenergy.2011.12.054.

[22] M. O'Grady, A.A. Lechowska, A.M. Harte, Infrared thermography technique as an in-situ method of assessing heat loss through thermal bridging, Energy Build. 135 (2017) 20–32, https://doi.org/10.1016/j.enbuild.2016.11.039.

[23] G. Baldinelli, et al., A model for the improvement of thermal bridges quantitative assessment by infrared thermography, 2017, pp. 854–864, Appl. Energy 211 (December) (2018), https://doi.org/10.1016/j.apenergy.2017.11.091.

[24] I. Nardi, E. Lucchi, T. de Rubeis, D. Ambrosini, Quantification of heat energy losses through the building envelope: A state-of-the-art analysis with critical and comprehensive review on infrared thermography, Build. Environ. 146 (July) (2018) 190–205, https://doi.org/10.1016/j.buildenv.2018.09.050.

[25] E. Lucchi, Applications of the infrared thermography in the energy audit of buildings: A review, 2017, pp. 3077–3090, Renew. Sustain. Energy Rev. 82 (July) (2018), https://doi.org/10.1016/j.rser.2017.10.031.

[26] M. Videras Rodríguez, S. G. Melgar, A. S. Cordero, and J. M. A. Márquez, "A Critical Review of Unmanned Aerial Vehicles (UAVs) Use in Architecture and Urbanism: Scientometric and Bibliometric Analysis," *Appl. Sci.*, vol. 11, no. 21, p. 9966, Oct. 2021, doi: 10.3390/app11219966.

[27] M.V. Rodríguez, S.G. Melgar, J.M.A. Márquez, Assessment of aerial thermography as a method of in situ measurement of radiant heat transfer in urban public spaces, Sustain. Cities Soc. no. October (2022) 104228, https://doi.org/10.1016/j.scs.2022.104228.

[28] M.V. Rodriguez, S.G. Melgar, J.M.A. Marquez, Design recommendations for the rehabilitation of an urban canyon in a subtropical climate region using aerial thermography and simulation tools, Energy Build. vol. 298, no. September (2023) 113525, https://doi.org/10.1016/j.enbuild.2023.113525.

[29] N. Bayomi, S. Nagpal, T. Rakha, J.E. Fernandez, Building envelope modeling calibration using aerial thermography, Energy Build. 233 (2021) 110648, https://doi.org/10.1016/j.enbuild.2020.110648.

[30] A. Benz, et al., Framework for a UAS-based assessment of energy performance of buildings, Energy Build. 250 (2021) 111266, https://doi.org/10.1016/j.enbuild.2021.111266.

[31] T. Rakha, A. Liberty, A. Gorodetsky, B. Kakillioglu, S. Velipasalar, Heat Mapping Drones: An Autonomous Computer-Vision-Based Procedure for Building Envelope Inspection Using Unmanned Aerial Systems (UAS), Technol. Archit. Des. 2 (1) (2018) 30–44, https://doi.org/10.1080/24751448.2018.1420963.

[32] European Committee for Standardization, ISO 6946:2017; Building components and building elements. Thermal resistance and thermal transmittance. Calculation method, 2017.

[33] D. Bienvenido-Huertas, J. Moyano, D. Marín, R. Fresco-Contreras, Review of in situ methods for assessing the thermal transmittance of walls, 2018, pp. 356–371, Renew. Sustain. Energy Rev. 102 (March) (2019), https://doi.org/10.1016/j.rser.2018.12.016.

[34] M. Teni, H. Krstić, P. Kosiński, Review and comparison of current experimental approaches for in-situ measurements of building walls thermal transmittance, Energy Build. 203 (2019), https://doi.org/10.1016/j.enbuild.2019.109417.

[35] I. Nardi, E. Lucchi, In situ thermal transmittance assessment of the building envelope: practical advice and outlooks for standard and innovative procedures, Energies, vol. 16, no. 8, 2023, doi: 10.3390/en16083319.

[36] F. Asdrubali, F. D'Alessandro, G. Baldinelli, F. Bianchi, Evaluating in situ thermal transmittance of green buildings masonries: A case study, Case Stud. Constr. Mater. 1 (2014) 53–59, https://doi.org/10.1016/j.cscm.2014.04.004.

[37] E. Lucchi, Thermal transmittance of historical brick masonries: A comparison among standard data, analytical calculation procedures, and in situ heat flow meter measurements, Energy Build. 134 (2017) 171–184, https://doi.org/10.1016/j.enbuild.2016.10.045.

[38] D.S. Choi, M.J. Ko, Comparison of various analysis methods based on heat flowmeters and infrared thermography measurements for the evaluation of the in situ thermal transmittance of opaque exteriorwalls, Energies, vol. 10, no. 7, 2017, doi: 10.3390/en10071019.

[39] European Committee for Standardization, *ISO 9869-1:2014; Thermal insulation. Building elements. Insitu measurement of thermal resistance and thermal transmittance. Part 1: Heat flow meter method.* 2014, p. 48.

[40] N. Soares, C. Martins, M. Gonçalves, P. Santos, L.S. da Silva, J.J. Costa, Laboratory and in-situ non-destructive methods to evaluate the thermal transmittance and behavior of walls, windows, and construction elements with innovative materials: A review, Energy Build. 182 (2019) 88–110, https://doi.org/10.1016/j.enbuild.2018.10.021.

[41] R. Walker, S. Pavía, Thermal performance of a selection of insulation materials suitable for historic buildings, Build. Environ. 94 (P1) (2015) 155–165, https://doi.org/10.1016/j.buildenv.2015.07.033.

[42] K. Gaspar, M. Casals, M. Gangolells, A comparison of standardized calculation methods for in situ measurements of façades U-value, Energy Build. 130 (2016) 592–599, https://doi.org/10.1016/j.enbuild.2016.08.072.

[43] G. Ficco, F. Iannetta, E. Ianniello, F.R. D'Ambrosio Alfano, M. Dell'Isola, U-value in situ measurement for energy diagnosis of existing buildings, Energy Build. 104 (2015) 108–121, https://doi.org/10.1016/j.enbuild.2015.06.071.

[44] L. Evangelisti, C. Guattari, R. De Lieto Vollaro, F. Asdrubali, A methodological approach for heat-flow meter data post-processing under different climatic conditions and wall orientations, Energy Build. 223 (2020) 110216, https://doi.org/10.1016/j.enbuild.2020.110216.

[45] P. Biddulph, et al., Inferring the thermal resistance and effective thermal mass of a wall using frequent temperature and heat flux measurements, Energy Build. 78 (2014) 10–16, https://doi.org/10.1016/j.enbuild.2014.04.004.

[46] European Committee for Standardization, ISO 8990:1997; Thermal insulation. Determination of steady-state thermal transmission properties. Calibrated and guarded hot box. 1997.
[47] F. Asdrubali, G. Baldinelli, Thermal transmittance measurements with the hot box method: Calibration, experimental procedures, and uncertainty analyses of three different approaches, Energy Build. 43 (7) (2011) 1618–1626, https://doi.org/10.1016/j.enbuild.2011.03.005.
[48] D. Bienvenido-Huertas, R. Rodríguez-Álvaro, J. J. Moyano, F. Rico, D. Marín, Determining the U-Value of fa ades using the thermometric method: Potentials and limitations, Energies, vol. 11, no. 2, 2018, doi: 10.3390/en11020360.
[49] L. Evangelisti, A. Scorza, R. De Lieto Vollaro, S.A. Sciuto, Comparison between heat flow meter (HFM) and thermometric (THM) method for building wall thermal characterization: latest advances and critical review, Sustain., vol. 14, no. 20, 2022, doi: 10.3390/su142013398.
[50] B. Mobaraki, F.J. Castilla Pascual, F. Lozano-Galant, J.A. Lozano-Galant, R. Porras Soriano, In situ U-value measurement of building envelopes through continuous low-cost monitoring, Case Stud. Therm. Eng., vol. 43, no. January, 2023, doi: 10.1016/j.csite.2023.102778.
[51] M. Domazetović, H. Krstić, D. Obradović, In-situ measurement and evaluation of thermal transmittance value by means of temperature-based method, Adv. Sci. Technol. Innov. (2021) 411–414, https://doi.org/10.1007/978-3-030-35533-3_49.
[52] J. M. Andújar Márquez, M. Á. Martínez Bohórquez, S. Gómez Melgar, A new metre for cheap, quick, reliable and simple thermal transmittance (U-Value) measurements in buildings, Sensors (Basel)., vol. 17, no. 9, 2017, doi: 10.3390/s17092017.
[53] S.H. Kim, J.H. Kim, H.G. Jeong, K.D. Song, Reliability field test of the air-surface temperature ratio method for in situ measurement of U-values, Energies 11 (4) (2018) 1–15, https://doi.org/10.3390/en11040803.
[54] European Committee for Standardization, *ISO 9869-2:2018; Thermal insulation. Building elements. Insitu measurement of thermal resistance and thermal transmittance. Part 1: Infrared method for frame structure dwelling.* 2018.
[55] I. Danielski, M. FrOling, Diagnosis of buildings' thermal performance-a quantitative method using thermography under non-steady state heat flow, Energy Procedia 83 (2015) 320–329, https://doi.org/10.1016/j.egypro.2015.12.186.
[56] B. Tejedor, M. Casals, M. Gangolells, Assessing the influence of operating conditions and thermophysical properties on the accuracy of in-situ measured U-values using quantitative internal infrared thermography, Energy Build. 171 (2018) 64–75, https://doi.org/10.1016/j.enbuild.2018.04.011.
[57] M. Mahmoodzadeh, V. Gretka, K. Hay, C. Steele, P. Mukhopadhyaya, Determining overall heat transfer coefficient (U-Value) of wood-framed wall assemblies in Canada using external infrared thermography, Build. Environ. vol. 199, no. May (2021) 107897, https://doi.org/10.1016/j.buildenv.2021.107897.
[58] B. Lehmann, K. Ghazi Wakili, T. Frank, B. Vera Collado, C. Tanner, Effects of individual climatic parameters on the infrared thermography of buildings, Appl. Energy 110 (2013) 29–43, https://doi.org/10.1016/j.apenergy.2013.03.066.
[59] R. Albatici, A.M. Tonelli, M. Chiogna, A comprehensive experimental approach for the validation of quantitative infrared thermography in the evaluation of building thermal transmittance, Appl. Energy 141 (2015) 218–228, https://doi.org/10.1016/j.apenergy.2014.12.035.
[60] G. Dall'O', L. Sarto, A. Panza, Infrared screening of residential buildings for energy audit purposes: Results of a field test, Energies 6 (8) (2013) 3859–3878, https://doi.org/10.3390/en6083859.
[61] R. Albatici, A.M. Tonelli, Infrared thermovision technique for the assessment of thermal transmittance value of opaque building elements on site, Energy Build. 42 (11) (2010) 2177–2183, https://doi.org/10.1016/j.enbuild.2010.07.010.
[62] X. Lu, A.M. Memari, Comparison of the experimental measurement methods for building envelope thermal transmittance, Buildings 12 (3) (2022) 1–15, https://doi.org/10.3390/buildings12030282.
[63] B. Tejedor, E. Barreira, Vasco peixoto de Freitas, T. Kisilewicz, K. Nowak-Dziesko, U. Berardi, Impact of stationary and dynamic conditions on the U-value measurements of heavy-multi leaf walls by quantitative IRT, Energies 13 (6611) (2020) 19.
[64] B. Tejedor, M. Casals, M. Gangolells, X. Roca, Quantitative internal infrared thermography for determining in-situ thermal behaviour of façades, Energy Build. 151 (2017) 187–197, https://doi.org/10.1016/j.enbuild.2017.06.040.
[65] M.H. Abdul Nasir, A.S. Hassan, Thermal performance of double brick wall construction on the building envelope of high-rise hotel in Malaysia, J. Build. Eng. vol. 31, no. April (2020) 101389, https://doi.org/10.1016/j.jobe.2020.101389.
[66] P.A. Fokaides, S.A. Kalogirou, Application of infrared thermography for the determination of the overall heat transfer coefficient (U-Value) in building envelopes, Appl. Energy 88 (12) (2011) 4358–4365, https://doi.org/10.1016/j.apenergy.2011.05.014.
[67] I. Nardi, S. Sfarra, D. Ambrosini, Quantitative thermography for the estimation of the U-value: State of the art and a case study, J. Phys. Conf. Ser., vol. 547, no. 1, 2014, doi: 10.1088/1742-6596/547/1/012016.
[68] I. Nardi, D. Paoletti, D. Ambrosini, T. De Rubeis, S. Sfarra, U-value assessment by infrared thermography: A comparison of different calculation methods in a Guarded Hot Box, Energy Build. 122 (2016) 211–221, https://doi.org/10.1016/j.enbuild.2016.04.017.
[69] M. Fox, D. Coley, S. Goodhew, P. De Wilde, Thermography methodologies for detecting energy related building defects, Renew. Sustain. Energy Rev. 40 (2014) 296–310, https://doi.org/10.1016/j.rser.2014.07.188.
[70] M. Mahmoodzadeh, V. Gretka, P. Mukhopadhyaya, Challenges and opportunities in quantitative aerial thermography of building envelopes, 2022, p. 106214, J. Build. Eng. 69 (October) (2023), https://doi.org/10.1016/j.jobe.2023.106214.
[71] M.C. Peel, B.L. Finlayson, T.A. McMahon, Updated world map of the Köppen-Geiger climate classification, Hydrol. Earth Syst. Sci. (2007), https://doi.org/10.5194/hess-11-1633-2007.
[72] A. Kirimtat, O. Krejcar, A review of infrared thermography for the investigation of building envelopes: Advances and prospects, Energy Build. 176 (2018) 390–406, https://doi.org/10.1016/j.enbuild.2018.07.052.
[73] Deutsche Institut für Normung e.V. (DIN), DIN 16714-3:2016-11; Non-destructive testing. Thermographic testing. Part 3: Terms and definitions. 2016.
[74] European Committee for Standardization, ISO 18434-1:2008; Condition monitoring and diagnostics of machines. Thermography. Part 1: General procedures. 2008.
[75] R. Madding, "Finding R-Values of Stud Frame Constructed Houses with IR Thermography," *Proc. ITC*, vol. 126, no. January 2008, pp. 2008–2013, 2008.
[76] K. Watanabe, Architectural Planning Fundamentals. (1965).
[77] D. Bienvenido-Huertas, J. Bermúdez, J. Moyano, D. Marín, Comparison of quantitative IRT to estimate U-value using different approximations of ECHTC in multi-leaf walls, Energy Build. 184 (2019) 99–113, https://doi.org/10.1016/j.enbuild.2018.11.028.
[78] C.J. Willmott, On the validation of models, Phys. Geogr. 2 (2) (1981) 184–194, https://doi.org/10.1080/02723646.1981.10642213.
[79] I. Nardi, D. Ambrosini, T. De Rubeis, S. Sfarra, S. Perilli, G. Pasqualoni, A comparison between thermographic and flow-meter methods for the evaluation of thermal transmittance of different wall constructions, J. Phys. Conf. Ser., vol. 655, no. 1, 2015, doi: 10.1088/1742-6596/655/1/012007.